

**Sesquiterpene lactones from *Geigeria aspera*:
isolation, cytotoxicity against murine muscle cell lines
and microsomal metabolism**

by

Yvette Zethu Mathe

Submitted in fulfilment of the requirements for the degree

Master of Science in Veterinary Science

in the Faculty of Veterinary Science

University of Pretoria

April 2020

Supervisor: Prof CJ Botha

Declaration of originality

By submitting this dissertation:

I declare that the work contained in this dissertation is original and has been carried out by me (save to the extent explicitly otherwise stated) in the Department of Paraclinical Sciences, Faculty of Veterinary Science. Reproduction and publication thereof by the University of Pretoria will not infringe any third party rights. No part of this dissertation was previously submitted for any other degree at any university.

Summary

Vermeersiekte or 'vomiting disease' is an economically important disease of ruminants following ingestion of *Geigeria* species in South Africa. Sheep are more susceptible and poisoning is characterised by stiffness, regurgitation, bloat, paresis and paralysis. *Geigeria aspera* was collected in the Vrede district (27° 25' 48" S; 29° 9' 36" E), Free State Province. The plant material was dried, milled and the toxic principles, known as sesquiterpene lactones, were extracted and isolated following chromatographic procedures. Even though geigerin and ivalin were previously isolated, an unknown sesquiterpene lactone, isogeigerin acetate, was also purified. Mouse myoblast (C2C12) and rat embryonic cardiac myocyte (H9c2) cell lines were exposed to different concentrations of geigerin, ivalin, isogeigerin acetate and a commercially available sesquiterpene lactone, parthenolide. An *in vitro* colorimetric assay 3-(4,5-dimethylthiazol-2-yl)-2,5-diphenyltetrazolium bromide (MTT) was used to assess cytotoxicity. The median effective concentrations (EC₅₀) indicated that ivalin and parthenolide were significantly ($p < 0.05$) more toxic than geigerin and isogeigerin acetate. A concentration-dependent cytotoxic response was observed in both cell lines, however, C2C12 cells were more sensitive. A high performance liquid chromatography (HPLC) analysis was used to evaluate the *in vitro* metabolism of parthenolide, following the addition of a mouse liver microsomal fraction. Results revealed that parthenolide, incubated with the microsomal fraction, undergoes enzymatic transformation to form a metabolite.

Keywords: *Geigeria aspera*, cytotoxicity, ivalin, geigerin, isogeigerin acetate, parthenolide, microsomal fraction.

Acknowledgements

- I foremost would like to thank my supervisor, Prof C.J. Botha, for giving me the opportunity to be part of this research and for his great support at all times, I am extremely grateful.
- Many thanks to the departmental laboratory technologists, Ms Annette Venter and Ms Arina Ferreira and organic chemist, Dr Gerda Fouché for their assistance throughout my project.
- Thanks for the statistical support of statistician, Ms Marie Smith, for assistance in results analysis.
- I would also like to thank the University of Pretoria for supporting me with a post-graduate research bursary.
- Not forgetting my family, especially my parents for motivating me to work harder and encouraging me to believe in the power of faith and self-belief.
- My lovely gratitude to my close friends, thank you so much.
- Jeremiah 29:11; “for I know the plans I have for you,” declares the LORD, “plans to prosper you and not to harm you, plans to give you hope and a future”.

Table of Contents

List of abbreviations	vii
List of figures	viii
List of tables	ix
List of equations	ix
Chapter 1: Introduction	1
1.1. Problem statement	2
1.2 Objectives	2
Chapter 2: Literature review	3
2.1. Toxicology	3
2.2 Genus <i>Geigeria</i>	4
2.2.1 <i>Geigeria</i> species	4
2.2.2 Description of <i>Geigeria aspera</i> (vermeerbos)	5
2.2.3 Species distribution.....	6
2.3 Vermeersiekte (Vomiting disease)	8
2.3.1 Clinical signs of vermeersiekte.....	8
2.3.2. Pathological lesions.....	9
2.4 Sesquiterpene lactones	11
2.5 <i>In vitro</i> experimentation	13
2.5.1 Cytotoxicity assays	14
2.5.1.1 MTT viability assay	14
2.5.2 <i>In vitro</i> metabolic studies with liver microsomes	15
2.5.2.1 Liver biotransformation	15
2.5.2.2 Microsomal fractions	17
2.5.2.3 HPLC analysis	17
Chapter 3: Materials and methods	19
3.1 Plant toxins	19
3.1.1 Extraction and isolation of sesquiterpene lactones from <i>Geigeria aspera</i>	19
3.1.2 Unknown sesquiterpene lactone identification	21
3.1.3 Parthenolide.....	21
3.2 Cell cultures	21

3.2.1 Chemicals, reagents and plastic ware	21
3.2.2 Cell lines	22
3.3 Exposure studies	23
3.4 Cytotoxicity assay	24
3.4.1. MTT cytotoxicity assay	24
3.5 Parthenolide metabolism	24
3.5.1 Liver microsomes	24
3.5.2 High performance liquid chromatography (HPLC)	25
3.6 Statistical analysis	25
Chapter 4: Results.....	27
4.1. Identification, spectrometry and stereochemical characterization of the unknown compound	27
4.1.1 Identity of unknown compound	27
4.1.2 Mass spectrometry	28
4.1.3 NMR spectrum	29
4.1.4 X-ray analysis	30
4.2. <i>In vitro</i> cytotoxicity of sesquiterpene lactones - ivalin, isogeigerin acetate, geigerin and parthenolide - in C2C12 and H9c2 cell lines.....	31
4.2.1 Cytotoxic effect of ivalin, isogeigerin acetate, geigerin and parthenolide in C2C12 cells.....	31
4.2.2 Cytotoxic effect of ivalin and parthenolide in H9c2 cells.	35
4.3. <i>In vitro</i> hepatic microsomal metabolism of parthenolide determined by HPLC	38
Chapter 5: Discussion	45
Chapter 6: Conclusions.....	53
Chapter 7: References.....	55

List of abbreviations

ABS	Absorbance
ANOVA	Analysis of variance
AST	Aspartate transaminase
ATCC	American Tissue Culture Collection
CYP/ CYP450	Cytochrome P450
DMEM	Dulbecco's modified Eagle's medium
DMSO	Dimethyl sulphoxide
EC ₅₀	Median effective concentration
EDTA	Ethylenediaminetetraacetic acid
ER	Endoplasmic reticulum
FCS	Foetal calf serum
FPP	Farnesyl pyrophosphate
GGT	Gamma-glutamyl transferase
HPLC	High performance liquid chromatography
HRESIMS	High-resolution electrospray ionisation mass spectrometry
LC/MS	Liquid chromatography/mass spectrometry
LD ₅₀	Median lethal dose
MTT	3-(4,5-Dimethylthiazol-2-yl)-2,5- diphenyltetrazolium bromide
NADPH	Nicotinamide adenine dinucleotide phosphate (reduced)
NMR	Nuclear magnetic resonance
PBS	Phosphate-buffered saline
SER	Smooth endoplasmic reticulum
Sp(p)	Species
TLC	Thin-layer chromatography
UV	Ultraviolet

List of figures

Figure 2.1: (a) and (b) <i>Geigeria ornativa</i> , a small woody plant	4
Figure 2.2: <i>Geigeria ornativa</i> growing on limestone soil in the Northern Cape Province of South Africa (Courtesy L.D. Snyman, ARC-OVR)	5
Figure 2.3: (a) <i>Geigeria aspera</i> branched shrub and (b) yellow flowerhead with linear sessile leaves	6
Figure 2.4: Areas in South Africa where <i>Geigeria</i> poisoning occurs (Botha and Venter, 2002)	7
Figure 2.5: Sheep ingesting <i>Geigeria burkei</i> Harv. subsp. <i>burkei</i> var. <i>hirtella</i> Merxm. in the Limpopo Province (Botha <i>et al.</i> , 1997)	7
Figure 2.6: Regurgitation of ingesta (“vomition”) through the mouth and nose	8
Figure 2.7: Radiograph taken after barium contrast fluid was dosed <i>per os</i> to visualise the enlargement of the thoracic oesophagus (mega-oesophagus) of affected sheep. (Courtesy of L.D. Snyman, ARC-OVR) (Snyman <i>et al.</i> , 2008)	9
Figure 2.8: Diameter of oesophagus, mega-oesophagus (left) compared to a normal oesophagus (right) (Courtesy of L.D. Snyman, ARC-OVR)	10
Figure 2.9: MTT assay reaction catalysed by mitochondrial dehydrogenase http://www.biopcr.com/Shop/cellbioch/60991.html	15
Figure 3.1: Ivalin	19
Figure 3.2: Geigerin	19
Figure 3.3: Schematic diagram of the extraction and isolation of ivalin, geigerin and the unknown sesquiterpene lactone.....	20
Figure 3.4: Parthenolide	21
Figure 4.1: Isogeigerin acetate	27
Figure 4.2: The ESI TOF mass spectrum of isogeigerin acetate	28
Figure 4.3: <i>MERCURY</i> drawing of the structure of isogeigerin acetate showing the stereochemistry of the molecule (Fouché <i>et al.</i> , 2019)	30
Figure 4.4: Logistic curves of the observed and fitted relationship following exposure of C2C12 myoblasts to ivalin for 24, 48 and 72 h	31
Figure 4.5: Exponential curves of the observed and fitted relationship following exposure of C2C12 myoblasts and H9c2 cardiac myocytes to isogeigerin acetate for 48 h	32
Figure 4.6: Exponential curves of the observed and fitted relationship following exposure of C2C12 myoblasts to geigerin for 24, 48 and 72 h	33
Figure 4.7: Logistic curves of the observed and fitted relationship following exposure of C2C12 myoblasts to parthenolide for 24, 48 and 72 h	34
Figure 4.8: Exponential curves of the observed and fitted relationship following exposure of H9c2 cardiac myocytes to ivalin for 24, 48 and 72 h	35
Figure 4.9: Exponential curves of the observed and fitted relationship following exposure of H9c2 cardiac myocytes to parthenolide for 24, 48 and 72h	36
Figure 4.10: HPLC chromatogram, only incubation buffer (blank)	38
Figure 4.11: HPLC chromatogram of only the microsomal fraction incubated in the buffer	39
Figure 4.12: Parthenolide (4.25 μ M) incubated without and with microsomal fraction	40
Figure 4.13: Parthenolide (6.25 μ M) incubated without and with microsomal fraction	40

Figure 4.14: Parthenolide (13.25 μM) incubated without and with microsomal fraction	41
Figure 4.15: Parthenolide (26.5 μM) incubated without and with microsomal fraction	41
Figure 4.16: Parthenolide (53 μM) incubated without and with microsomal fraction	42
Figure 4.17: Overlay of HPLC chromatograms of parthenolide incubated at increasing concentrations (4.25, 6.625, 13.25, 26.5 and 53 μM) with the microsomal fraction	43
Figure 4.18: Metabolism of parthenolide after incubation with the microsomal fraction as detected by HPLC....	44
Figure 4.19: Linear relationship of parthenolide at increasing concentrations, incubated without and with the microsomal fraction, and the metabolite as detected by HPLC.....	44

List of tables

Table 4.1. NMR spectroscopic data for isogeigerin acetate	29
Table 4.2: EC_{50}s of ivalin, isogeigerin acetate, geigerin and parthenolide determined on C2C12 and H9c2 cells after 24, 48 and 72 h exposure times.....	37
Table 4.3: Parthenolide incubated without and with microsomal fraction	44

List of equations

Equation 1: Calculation of cell number using a haemocytometer	22
Equation 2: Calculation of percentage cell viability (blank: incubation medium, control: cells incubated in medium).....	23

Chapter 1: Introduction

The plant poisoning vermeersiekte (Rimington *et al.*, 1936), also referred to as “vomiting disease” (Van Heerden *et al.*, 1993), is caused by several *Geigeria* species. It affects ruminants, mainly sheep, after ingestion of sufficient quantities of *Geigeria* plant material. *Geigeria aspera* is more toxic than other *Geigeria* species. The degree of toxicity of the plant is location dependent where soil type and climatic conditions play a role (Steyn, 1930). Several sesquiterpene lactones, e.g. vermeeric acid, geigerin and geigerinin have been isolated from *Geigeria* species (Grosskopf, 1964; Kellerman *et al.*, 2005). Between 1929-1930, vermeersiekte caused the deaths of millions of sheep in the Griqualand West region of the Northern Cape Province of South Africa (Vahrmeijer, 1981). Kellerman *et al.* (1996) estimated the monetary value of annual mortalities and production and reproduction losses attributed to vermeersiekte, at that time, at 6 million Rand. Outbreaks of this disease have been reported periodically from the Northern Cape, Free State, North-West and Mpumalanga provinces of South Africa. Therefore, vermeersiekte is an economically important plant poisoning of small stock in South Africa (Kellerman *et al.*, 1996).

Clinically, four forms of the disease are recognised; i.e. stiffness, paralysis, regurgitation (which can lead to asphyxiation or foreign body pneumonia) and bloating. Treatment of affected sheep was attempted by using cysteine and piracetum, but was largely unsuccessful (Joubert, 1983). Other management practices to prevent intoxication include tactical grazing (such as rotational grazing), removal of plants from the grazing camps (Kellerman *et al.*, 2005), conditioned feed aversion (Snyman *et al.*, 2002) and improved pasture management (Kellerman *et al.*, 1996).

This research project elucidated the chemical structure of the unknown sesquiterpene lactone, that was isolated and purified from *Geigeria aspera* in the departmental laboratory, as isogeigerin acetate (Fouché *et al.*, 2019). Subsequently, the cytotoxicity caused by the three *G. aspera* sesquiterpene lactones; i.e. ivalin, geigerin and isogeigerin acetate; was compared to a commercially available sesquiterpene lactone, parthenolide. *In vitro* studies were conducted using two commercial cell lines; i.e. mouse skeletal myoblasts (C2C12) and rat embryonic cardiac myocytes (H9c2). The *in vitro* cytotoxicity of different concentrations

of the sesquiterpene lactones, after various exposure periods, was determined. In addition, the biotransformation of parthenolide, a highly toxic sesquiterpene lactone, was evaluated by the addition of a mouse liver microsomal extract, enriched for Phase I cytochrome P450 metabolic enzymes capable of catalysing oxidation, reduction and hydrolysis reactions.

1.1 Problem statement

Little is known about the difference in toxicity of the various sesquiterpene lactones and their individual contribution to the above-mentioned clinical signs. The role that biotransformation of these compounds, in the liver following gastrointestinal absorption, plays in their ultimate and interactive toxicity is also still unknown. The interactive toxicity, e.g. additive or synergistic effects of different sesquiterpene lactones or sesquiterpene lactones with their metabolites has not been studied.

1.2 Objectives

There were a number of objectives formulated.

- Elucidate the chemical structure of isogeigerin acetate with the aid and guidance of an organic chemist.
- Determine the cytotoxic effect of ivalin, isogeigerin acetate, geigerin and parthenolide on the C2C12 cell line using the 3-(4,5-dimethylthiazol-2-yl)-2,5-diphenyltetrazolium bromide MTT assay.
- Determine the cytotoxic effect of ivalin, isogeigerin acetate and parthenolide on the H9c2 cell line using the MTT assay.
- Investigate if parthenolide is metabolised, following the addition of a microsomal fraction, using high performance liquid chromatography (HPLC).

Chapter 2: Literature review

2.1 Toxicology

Toxicology is the study of chemicals and their association with biological systems to produce harmful effects in living organisms. To cause an effect, a toxic substance must first be exposed to the skin; mucosa of the eye; or mucosa of the respiratory tract and alimentary canal through inhalation or ingestion, respectively. The severity of the reaction will be dependent on exposure, absorption, distribution, metabolism and presence of protective mechanisms and excretion (Timbrell, 2008).

Plant poisonings depend on the type of phytotoxin ingested as well as the species, breed, sex, age, etc. of the animal. An animal's physical condition and nutritional state, such as hunger caused by shortage of grazing due to drought, veld fires, unpalatability and overgrazing, can lead to ingestion of accessible poisonous plants (Knight, 2007). The availability and abundance of plants, prevailing climatic conditions and/or pasture management are all factors that influence exposure of livestock to toxic plants (Penrith *et al.*, 2015).

Poisoning by plants has an economic impact on livestock production in South Africa. Monetary losses from plant poisoning can be ascribed to either direct or indirect losses. Direct losses consist of mortalities, diminished body mass and reproductive failures such as decreased libido, infertility, birth defects, abortions, stillbirths and/or protracted gestation. Whereas indirect losses include the cost of management practices such as supplementary feeding, fencing for strategic grazing, as well as treatment costs (Kellerman *et al.*, 1996).

Losses in small stock, primarily in sheep, are caused by some major plant poisonings namely, geeldikkop (*Tribulus terrestris*), cardiac glycoside poisoning (e.g. *Tylecodon wallichii*), seneciosis (*Senecio* species), gousiekte (e.g. *Pachystigma pygmaeum* [= *Vangueria pygmaea*]) and vermeersiekte (*Geigeria* species) (Kellerman *et al.*, 1996).

2.2 Genus *Geigeria*

2.2.1 *Geigeria* species

The genus *Geigeria* is a member of the Asteraceae family, an angiosperm family well known as flowering plants (Meyer and Van Staden, 1989). Within South Africa *Geigeria* is considered as one of the six most important poisonous plant species (Kellerman *et al.*, 1996; Pienaar *et al.*, 1973). There are numerous species reported to be toxic, such as *Geigeria aspera*, *G. burkei*, *G. ornativa* (Figure 2.1 a, b) and *G. pectidea* (Kellerman *et al.*, 2005). The *Geigeria* species most often incriminated for causing intoxication are *Geigeria aspera* and *G. ornativa*, with *G. aspera* 10 times more toxic than *G. ornativa* (Kellerman *et al.*, 2005).

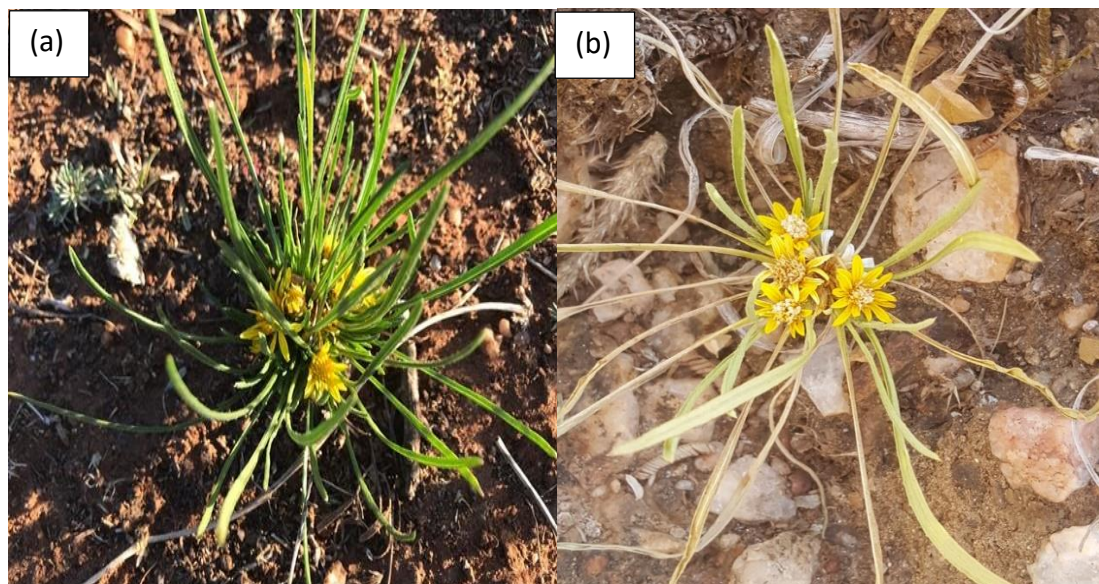


Figure 2.1: (a) and (b) *Geigeria ornativa*, a small woody plant.

Toxicity of plants vary during different seasons of the year and locality (Kellerman *et al.*, 2005). Van Heerden *et al.* (1993) also listed other factors including soil type and developmental stages of the plant as contributing to the variation in toxicity. For instance, when the plant is growing on limestone it is most toxic (Figure 2.2.) (Steyn, 1934).



Figure 2.2: *Geigeria ornativa* growing on limestone soil in the Northern Cape Province of South Africa (Courtesy L.D. Snyman, ARC-OVR).

2.2.2 Description of *Geigeria aspera* (vermeerbos)

Geigeria aspera (also referred to as *G. aspera* Harv. var. *aspera*) is a dense woody shrublet, with several small yellow flowers (Figure 2.3 a, b). The flowering season is from the end of October to the end of April (Meyer and Van Staden, 1989; Vahrmeijer, 1981). There are both unisexual (female) and bisexual florets, borne in dense heads in the leaf-axils or ends of branches (Vahrmeijer, 1981). Their erect leaves are rough in texture and closely arranged on the branches and are approximately 4 mm wide and 6 cm long (Vahrmeijer, 1981). After flowering and once the flowerhead bracts have decayed, they release slender seeds. Approximately 1900 seeds are dispersed from the plant, they remain viable for a long period (at least 13 years) and germinate under favourable conditions (Vahrmeijer, 1981).

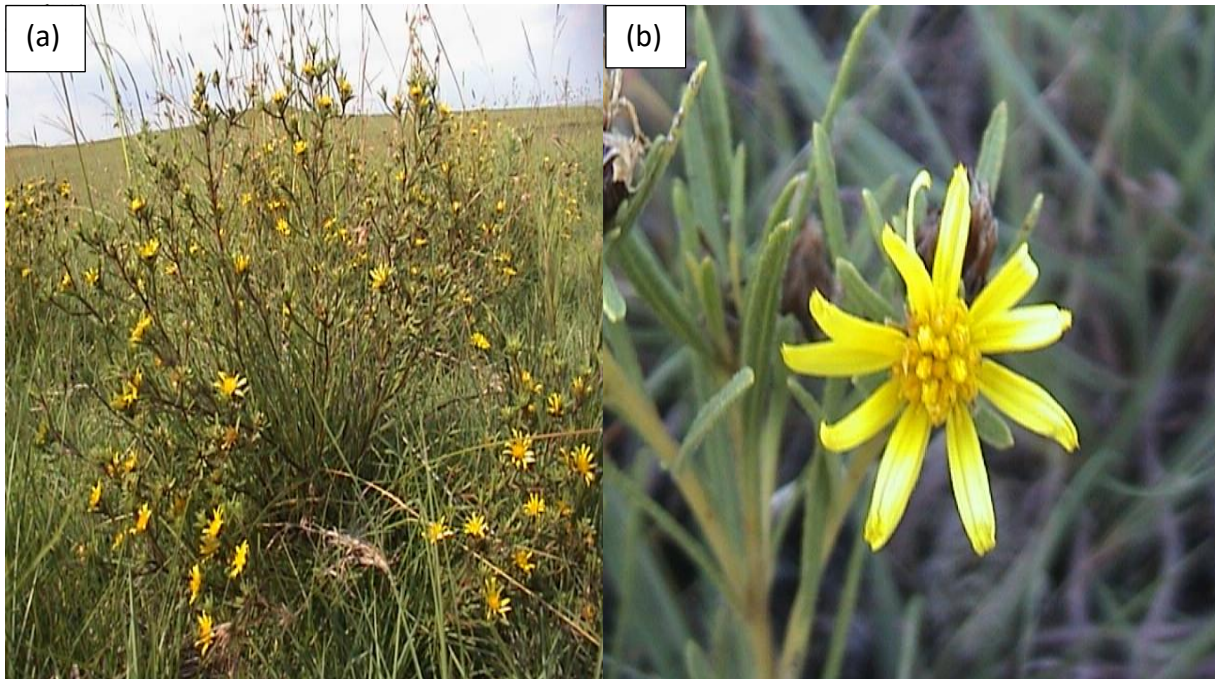


Figure 2.3: (a) *Geigeria aspera* branched shrub and (b) yellow flowerhead with linear sessile leaves.

2.2.3 Species distribution

Geigeria aspera occurs over the southern part of Africa, exclusively in the South African eastern Highveld, in moist savannah regions with high rainfall areas close to riverbanks or swamps and grows in loam and clay soils in over-grazed veld (Botha and Venter, 2002; Meyer and Van Staden, 1989). The areas where poisoning with *Geigeria* species are reported are depicted in Figure 2.4 and massive losses of livestock have also been recorded in Namibia (Rimington *et al.*, 1936).

Geigeria ornativa occurs in the drier, semi-arid parts of the southern, south-western and western parts of South Africa and in Namibia commonly on calciferous soils. Large outbreaks occurred in the Griqualand West area of the Northern Cape Province during 1929-1930 (Kellerman *et al.*, 2005; Vahrmeijer, 1981).

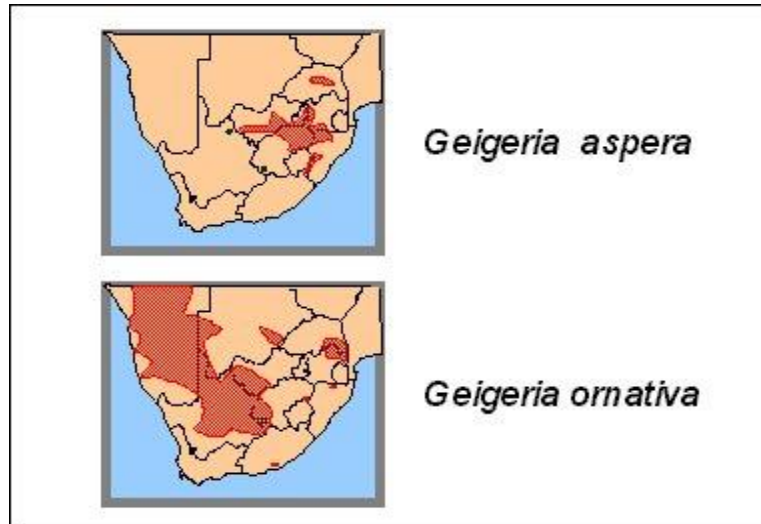


Figure 2.4: Areas in South Africa where *Geigeria* poisoning occurs (Botha and Venter, 2002).

G. burkei subsp. *burkei* occurs in Limpopo, North-West, Gauteng, Mpumalanga and Free State provinces of South Africa (Retief, 2003) and an outbreak ascribed to *Geigeria burkei* subsp. *burkei* var. *hirtella* was recorded at Bandolierskop, Limpopo Province (Figure 2.5) (Botha *et al.*, 1997).



Figure 2.5: Sheep ingesting *Geigeria burkei* Harv. subsp. *burkei* var. *hirtella* Merxm. in the Limpopo Province (Botha *et al.*, 1997).

2.3 Vermeersiekte (Vomiting disease)

Vermeersiekte is common in sheep (Steyn, 1930; Van Heerden *et al.*, 1993), but it also occurs in goats and cattle (Kellerman *et al.*, 2005). The susceptibility of an animal depends on its nutritional state, where particularly young and pregnant animals, ewes with lambs and heavy wool producers have the highest nutritional demand (Kellerman *et al.*, 2005; Vahrmeijer, 1981).

2.3.1 Clinical signs of vermeersiekte

After ingestion of plant material over an extended period (approximately 3 weeks with *G. ornativa*), clinical signs are noticed (Kellerman *et al.*, 2005). Affected sheep walk with a stiff gait, fatigue sets in and they lag behind the flock. The animals loose condition. The muzzle can be tinged with a greenish blotch, as the animal regurgitates ingesta (“vomition”) at irregular intervals as illustrated in Figure 2.6 (Kellerman *et al.*, 2005).



Figure 2.6: Regurgitation of ingesta (“vomition”) through the mouth and nose

With progression of the disease, the animals stand with an arched back, collapse and become paralysed (Van Heerden *et al.*, 1993). According to Kellerman *et al.* (2005) clinically, four forms of the disease are recognised; i.e. stiffness, paralysis, regurgitation (due to severe oesophageal dilation, the so-called mega-oesophagus [Figure 2.7]) and bloating. Animals may exhibit one or more of the clinical forms as described above (Pienaar *et al.*, 1973). Mortalities

due to vermeersiekte have been attributed to asphyxiation, foreign body pneumonia, paralysis of the respiratory centre, exhaustion and cardiac failure (Van Heerden *et al.*, 1993).



Figure 2.7: Radiograph taken after barium contrast fluid was dosed *per os* to visualise the enlargement of the thoracic oesophagus (mega-oesophagus) of affected sheep. (Courtesy of L.D. Snyman, ARC-OVR) (Snyman *et al.*, 2008).

Differential diagnosis of vermeersiekte includes botulism (“lamsiekte”), krimpsiekte (“shrinking disease”), diplodiosis, ephemeral fever (three-day-stiff sickness), laminitis and fluorosis (Kellerman *et al.*, 2005).

2.3.2. Pathological lesions

At necropsy an increased oesophageal diameter may be evident with consistent dilation, the so-called mega-oesophagus (Figure 2.8) (Kellerman *et al.*, 2005; Snyman *et al.*, 2008) and signs of foreign body pneumonia might be present in the apical and cardiac lobes of the lungs (Kellerman *et al.*, 2005).



Figure 2.8: Diameter of oesophagus, mega-oesophagus (left) compared to a normal oesophagus (right) (Courtesy of L.D. Snyman, ARC-OVR).

Microscopical evaluation of natural and experimentally-induced vermeersiekte cases revealed changes in the skeletal and oesophageal muscles (Pienaar *et al.*, 1973; Van der Lugt and Van Heerden, 1993). Histologically, skeletal, diaphragm and oesophageal myofibres were atrophic and degenerated with myofibre vacuolisation (Pienaar *et al.*, 1973; Van der Lugt and Van Heerden, 1993). Furthermore, damaged myofibres had dissimilar sized vacuoles, with one or more intruded nuclei and exhibited hyalinisation (Kellerman *et al.*, 2005). Van der Lugt and Van Heerden (1993) identified myofibrillar degeneration and mitochondrial swelling in the myocardium, semimembranosus muscle and oesophagus. Firstly, thick myosin filaments disappeared resulting in interruption of the A-band, then the loss of the actin-thin filaments followed by myofibrillar lysis. The Z-band was thickened, fragmented or tortuous and accompanied with altered mitochondria (Pienaar *et al.*, 1973; Van der Lugt and Van Heerden, 1993).

In addition to the muscle pathology, degeneration of hepatocytes with elevated levels of aspartate transaminase (AST) and gamma-glutamyl transferase (GGT) were detected in the sera of sheep, which confirmed some liver damage (Botha *et al.*, 1997; Kellerman *et al.*, 2005).

2.4 Sesquiterpene lactones

Lipophilic compounds, known as sesquiterpene lactones, are believed to cause vermeerziekte (Botha *et al.*, 2017; Kellerman *et al.*, 2005). There are several sesquiterpene lactones that have been extracted, purified and identified from *Geigeria* species such as geigerin, geigerinin, ivalin, vermeerin and dihydrogriesenin (Meyer and Van Staden, 1986; Rimington and Roets, 1936; Rimington *et al.*, 1936; Vogelzang *et al.*, 1978). These colourless stable compounds are biosynthesised by plants from isoprene, via farnesyl pyrophosphate (FPP), within the endoplasmic reticulum (ER) (Meyer and Van Staden, 1986). The majority of sesquiterpene lactones originate from genera belonging to the Asteraceae family (Picman, 1986; Rodriguez *et al.*, 1976). They are differentiated based on the structure of their carbocyclic skeleton (Meyer and Van Staden, 1986; Rodriguez *et al.*, 1976). They have a basic structure that contains 15 carbon atoms, an active gamma(γ)-lactone ring at either carbon-6 or carbon-8, mostly containing the α -methylene group, thus referred as a α -dimethene- γ -lactone group (Chadwick *et al.*, 2013; Padilla-Gonzalez *et al.*, 2016).

These compounds are toxic to animals, vertebrates, humans and insects (Picman, 1986); whilst in humans they may also cause an allergic dermatitis (Gaspar *et al.*, 1986). The cytotoxic effect of the sesquiterpene lactones can be ascribed to the exo-methylene group of the carbocyclic skeleton (Picman, 1986). Cytotoxicity of sesquiterpene lactones can be reduced by the saturation of/or addition to the methylene group. On the other hand, cytotoxicity can be enhanced by the addition of a conjugated ester, cyclopentenone, lactone, epoxy group or steric hindrance (Picman, 1986). Kupchan *et al.* (1971) stipulated that an increase in lipophilicity leads to an increase in cytotoxicity.

Toxicity of sesquiterpene lactones may be correlated with their molecular structural arrangement, reactive sites, steric hindrance and/or presence of functional groups (Patnaik, 2007) such as the methyl (CH₃) and methylene (CH₂) exocyclic groups (Hussien *et al.*, 2016). Their structure-cytotoxic activity relationship consists of the α -methylene- γ -lactone group (Rossi *et al.*, 1986) that undergoes a Michael reaction with enzymes, proteins, etc. accepting and reacting with nucleophiles like sulfhydryl or amino groups (Ivanescu *et al.*, 2015) resulting in an alkylation process that leads to altered biological functions (Narasimhan *et al.*, 1989).

Sesquiterpene lactones are inhibitors of mitochondrial respiration, glycolytic enzymes, nucleic acid synthesis, tumor growth (Gaspar *et al.* 1986; Rodriguez *et al.* 1976; Van Aswegen *et al.*, 1979; Van Aswegen *et al.*, 1982) and oxygen uptake during oxidative phosphorylation (Narasimhan *et al.*, 1989). According to Rodriguez *et al.* (1976) and Narasimhan *et al.* (1989) the presence of highly electrophilic functional groups and alkylation of critical enzymes or proteins results in that inhibitory action. Due to their hydrophobic nature, sesquiterpene lactones can penetrate both plasma and subcellular membranes of cells via the thiol groups and unsaturated ketone moieties present in the compound. This will facilitate covalent binding to critical proteins and enzymes, through the Michael addition mechanism, resulting in inhibition of mitochondrial oxidative phosphorylation (Kupchan *et al.*, 1971).

The inhibitory action of mitochondrial respiration is extensive, considering that the mitochondrial electron transport is inhibited at both coupling sites I and II (Narasimhan *et al.*, 1989). In addition, these compounds further inhibit the activities of choline dehydrogenase of the respiratory chain and pyruvate carboxylase complexes (Van Aswegen *et al.*, 1982). Furthermore, the number of alkylating moieties present in the molecule is related to their toxicity (Narasimhan *et al.*, 1989).

Botha *et al.* (2019) evaluated the effect of geigerin on desmin, an intermediate filament of the cytoskeleton. Desmin, a muscle-specific intermediate filament, fulfils an important role in maintaining the cytoskeletal architecture and cell structure (Costa, 2014). Disorganisation and loss of desmin were noticed after exposure of C2C12 cells to increasing concentrations of geigerin. The authors concluded that the disorganisation and aggregation of desmin filaments might play a pivotal role in the pathogenesis of vermeersiekte (Botha *et al.*, 2019).

2.5 In vitro experimentation

Scientific and technological advancement, as well as animal ethics, had led to the development and need for *in vitro* toxicity testing. An acute toxicity test, conducted in laboratory animals, called the classical LD₅₀ was developed with the premise to safeguard consumers and to select a safe dosage of xenobiotics (pharmaceuticals, food ingredients, chemicals and industrial products) for humans (Litchfield and Wilcoxon, 1949). An LD₅₀ is the dose of a test compound that will cause 50 percent mortalities in a uniform population of animals under controlled conditions. At first the determination of the LD₅₀ required large numbers of animals, but over the years' alternative approaches for reduction, refinement and replacement (3R's) were employed to curtail or abolish the unnecessary suffering and/or sacrifice of animals (Erhirhie *et al.*, 2018). Replacement tests encompasses *in vitro* tests using tissues and cells and *in silico* tests utilizes computer models to predict the effect of chemicals on humans and animals (Erhirhie *et al.*, 2018).

In vitro studies can be conducted on various constituents and tissues obtained from animals; i.e. isolated enzymes, subcellular fractions, transgenic cell lines, primary cell cultures, tissue slices and organs. The closer the experimental model resembles the basic building blocks of an organism the more affordable, available and ethically acceptable it becomes, but unfortunately its *in vivo* resemblance is also reduced accordingly (Brandon *et al.*, 2003). To lessen the gap between *in vitro* and *in vivo* experimentation, measures should be taken, where possible, to synchronise *in vitro* and *in vivo* studies (Nickien *et al.*, 2018). Computational models can be used to apply *in vitro* results to *in vivo* models and *vice versa* (Nickien *et al.*, 2018). A structured approach should also be followed when planning individual *in vitro* experiments to facilitate the logical integration of findings to predict *in vivo* effects and/or to elucidate the mechanisms of interference of xenobiotics with biological processes *in vivo* (Jia and Liu, 2007). *In vitro* studies are often used to optimise test conditions for further *in vivo* experimentation or to prevent the unnecessary suffering of animals in additional pointless and wasteful *in vivo* studies (Brandon *et al.*, 2003).

2.5.1 Cytotoxicity assays

Rapid, cheap, reliable, and reproducible cytotoxicity or cell viability assays are available to determine the cause of cell death. One of the classifications that can be used for these assays are based on the measurement of endpoints. Dye exclusion assays measure the intactness of the cell membrane of viable cells. On the other hand, colorimetric, fluorometric or luminometric assays measure uptake of dyes or the binding of dyes to DNA and proteins of viable cells or metabolic activity of viable cells (Aslantürk, 2018). Even though these assays do not require the use of animals, they cannot replace animal testing entirely, since intricate, interdependent biological processes cannot be mimicked at the cellular and subcellular level (Aslantürk, 2018). To obtain reliable and accurate results for a study, it is important to select an appropriate assay (Méry *et al.*, 2017). Therefore, for assays using cultured cells, a MTT colorimetric assay, monitoring the activity of omnipresent basal cellular enzymes, i.e. mitochondrial dehydrogenases, is valuable to determine the viability of remaining cells (Ahmed *et al.*, 1994).

2.5.1.1 MTT viability assay

Mossman (1983) developed the MTT assay to measure survival and proliferation of mammalian cells. The quantitative colorimetric assay is based on the reduction of a soluble yellow MTT dye, by mitochondrial dehydrogenases of viable cells, to an insoluble purple (dark) formazan product as represented in Figure 2.9. The nicotinamide adenine dinucleotide phosphate (NADPH)-dependent mitochondrial enzymes, defined as oxidoreductases, reduce the yellow tetrazolium dye, but is dependent on metabolic activity of viable cells. This assay thus also indicates the metabolic state of the cells (Kuetze *et al.*, 2017).

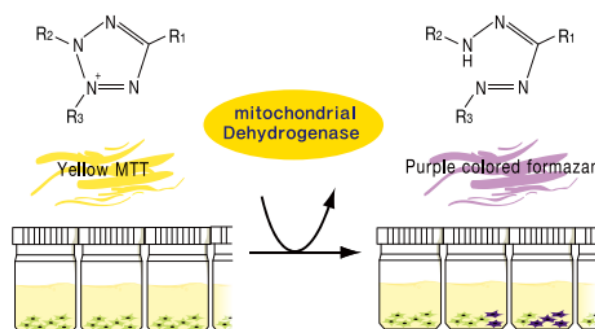


Figure 2.9: MTT assay reaction catalysed by mitochondrial dehydrogenase
<http://www.biopcr.com/Shop/cellbioch/60991.html>.

The rate of cell proliferation has a direct proportional relationship with the formazan product formed, therefore, a reduction in cell proliferation is indicated by lower absorbance (ABS) values. The MTT reagent is sensitive to light, therefore, the assay is performed in the dark (Ahmed *et al.*, 1994; Mossman, 1983). The insoluble formazan crystals are dissolved in DMSO (dimethyl sulphoxide) and the viable cells quantified in terms of intensity of the ABS of the formazan read at 570 nm with a reference wavelength of 630 nm.

2.5.2 In vitro metabolic studies with liver microsomes

2.5.2.1 Liver biotransformation

Following ingestion, a toxic substance is absorbed into the portal vein and then the central circulation, although a direct toxic effect at the exposed contact site may occur. Absorbed toxins are biotransformed by the liver, e.g. lipophilic xenobiotics can be metabolised to water-soluble substances, which contribute to the pre-systemic and the systemic elimination of many toxins (Roberts *et al.*, 2014). Lipophilic substances are poorly excreted and following biliary excretion they might be reabsorbed from the gastrointestinal tract (Timbrell, 2008). For complete elimination from the body a lipophilic toxin is usually metabolised by the liver to a water-soluble compound via Phase 1 and Phase 2 enzymes (Timbrell, 2008). In Phase 1 reactions the lipophilic foreign substance is modified by the addition of a functional group, which can change its chemical activity. During Phase 2 reactions the modified compound is conjugated to another chemical compound, such as glucuronic acid, to make it water soluble and easier to excrete, often via the kidneys. These reactions can occur sequentially, independently or simultaneously (Taxak and Bharatam, 2014).

Phase 1 enzymes are mainly cytochrome P450 (CYP450) mono-oxygenases. The CYP450 enzymes are responsible for biotransformation of foreign substances (Ogu and Maxa, 2000) and are located in the smooth endoplasmic reticulum (SER). CYP450 enzymes are present in the liver, however, they are also found in other tissues such as the intestinal tract, lung and kidney (Gonzalez and Tukey, 2006; Stavropoulou *et al.*, 2018). Apart from CYP450 mono-oxygenases (the major group of metabolising enzymes of xenobiotics) other enzymes responsible for methylation, acetylation, glucuronidation, sulphation and de-esterification also play an important role (Jia and Liu, 2007).

CYP450 isozymes *viz.* CYP1A2, CYP2C19, CYP2C9, CYP2D6, CYP2E1 and CYP3A4 are well known for biotransformation reactions, but CYP3A4 enzymes are recognised to metabolise most xenobiotics (Ogu and Maxa, 2000). CYP450 enzymes add hydroxyl, carboxyl or amino reactive groups through oxidation, reduction or hydrolysis reactions (Wu and McKown, 2004). The most common reaction is oxidation, during which the polar OH-group is introduced at several sites of the substrate, using a co-factor, NADPH, as a source of electrons for the substrate to be oxidised (Gonzalez and Tukey, 2006).

Xenobiotics can act as enzyme substrates, but also as inducers or inhibitors, thus affecting the rate of metabolism (Gonzalez and Tukey, 2006). Reduction of the substrate comprises the generation of hydroxyl or amino polar groups and hydrolysis entails the cleavage of chemical bonds of the substrate thereby changing the chemical properties of the substrate. These reaction mechanisms may vary because of the presence of sulphur, nitrogen and alkyl-, alkene- and phenyl groups (Taxak and Bharatam, 2014), thus influencing foreign substance activation or inactivation. Changes in the chemical structure of a parent compound might give rise to metabolite(s) with enhanced or reduced pharmacological or toxicological activities (Ogu and Maxa, 2000; Timbrell, 2008), which are removed from the body through renal and biliary excretion (Kok-Yong and Lawrence, 2015). The rate of the enzymatic reaction is described by the Michaelis-Menten first and zero order elimination kinetics. Elimination rate in first order kinetics is concentration dependent, whereas in zero order kinetics, elimination rate is independent of concentration; therefore, enzymes become saturated at higher drug concentrations resulting in a constant reaction rate (Jia and Liu, 2007). Hostanska *et al.* (2014) proposed that the biological activity of plant-derived preparations is influenced by the interference of CYP450 enzymes with the extracts.

2.5.2.2 Microsomal fractions

The microsomal fraction, enriched for the Phase 1 enzymes, and S9 fractions, enriched for Phase 1 and Phase 2 metabolic enzymes, are both prepared by differential centrifugation of a liver homogenate (Timbrell, 2008). For *in vitro* studies, the metabolic stability of a toxin can be evaluated by using commercially available liver microsomes (Wu and McKown, 2004). The liver microsomes contain cytochrome P450 enzymes that play an important role, utilising co-factors such as NADPH, in Phase 1 reactions. The metabolism depends on NADPH

concentration and incubation time and may produce more than one metabolite (Szultka-Mlynska and Buszewski, 2016). To obtain reproducible results, it is important to use the same source of liver microsomes to mimic *in vivo* conditions (Wu and McKown, 2004).

Various analytical techniques are used to determine if metabolism has occurred. Chromatographic techniques such as high performance liquid chromatography (HPLC), thin layer chromatography (TLC) and liquid chromatography/mass spectrometry (LC/MS) are used (Wu and McKown, 2004). For a fast, sensitive technique, HPLC can be used; however, compounds with similar ultraviolet (UV) spectra and elution times are difficult to be identified. LC/MS is more sensitive as it can also detect the specific mass of the analyte. TLC is simple, inexpensive and small volumes of samples are required, however, it has a lower separation efficiency than HPLC and LC/MS (Bertoli *et al.*, 2010; Lim and Lord, 2002).

2.5.2.3 HPLC analysis

High performance liquid chromatography (HPLC) is a technique for qualitative as well as quantitative analytical studies that can be completed at a relatively fast rate, with good resolution and sensitivity for separation of components in a mixture (Dong, 2006; Weon *et al.*, 2013). A fixed volume of the sample, in a liquid form, is applied to the column, by an automatic sample injector, for analysis. The components of the sample are distributed between the stationary (absorbent) phase and the liquid mobile phase carrying the components of mixture through the chromatography system according to their charge (Dong, 2006). HPLC techniques can either be normal or reversed-phase chromatography. Normal phase HPLC is based on a hydrophilic stationary phase with a non-polar mobile phase for separation of polar compounds, whereas reverse phase HPLC is based on a hydrophobic stationary phase and polar mobile phase, resulting in the separation of the components based on their interaction with absorbent particles (Nagy *et al.*, 2017).

Organic molecules such as amino acids, lipids, carbohydrates as well as ions, polymers or biomolecules are compounds suitable for HPLC analyses. The nature of their separation is based on molecular characteristics, affinity and/or differences in molecular weights. Thus, molecules with dissimilar polarity to the column are eluted faster whereas those with similar polarity move slower and stay longer on the chromatographic column (reflected as longer

retention times), hence compounds are eluted based on their polarity (Coskun, 2016; Petrova and Sauer, 2017).

The retention time is used for identification of separated compounds, represented as bands by the chromatogram. It is commonly measured in minutes and time taken for the compound to be eluted is a representation of its specific characteristic (Moldoveanu and David, 2013). Factors such as mobile phase composition, stationary phase, flow rate, chromatographic column dimensions and analyte functional groups can all result in retention time shifts. Therefore, it is mandatory to calibrate your HPLC apparatus to ensure that it is generating reproducible results (Gowrisankar *et al.*, 2010; Moldoveanu and David, 2013). An internal standard, a known concentration of a compound that is carefully selected, is used to improve the precision and accuracy of results. The amount to be added to sample and standard solutions should be calculated accurately to minimise errors (Hansen *et al.*, 2015). Furthermore, in an external standard calibration method, only the analyte is run at different concentrations to generate a standard curve. A calibration curve is generated by plotting the absolute analyte response against the analyte concentration usually at different concentrations (Moosavi and Ghassabian, 2018).

Chapter 3: Materials and Methods

3.1 Plant toxins

3.1.1 Extraction and isolation of sesquiterpene lactones from *Geigeria aspera*

Geigeria aspera was collected in the Vrede district (27° 25' 48" S; 29° 9' 36" E), Free State Province, Republic of South Africa. The plant material was dried and milled. The known sesquiterpene lactones, ivalin (Figure 3.1) and geigerin (Figure 3.2), as well as an unknown, sesquiterpene lactone were isolated and purified in the Pharmacology and Toxicology Laboratory, Department of Paraclinical Sciences, Faculty of Veterinary Science, using chromatographic procedures. This was part of a larger research project and the extraction and isolation processes are only summarised in Figure 3.3 (Fouché *et al.*, 2019).

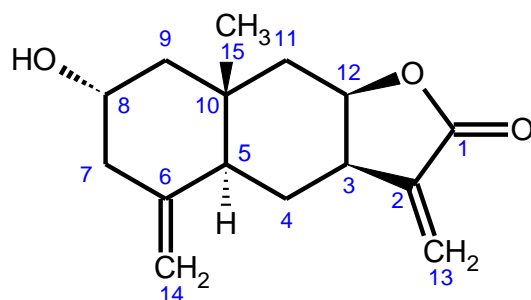


Figure 3.1: Ivalin

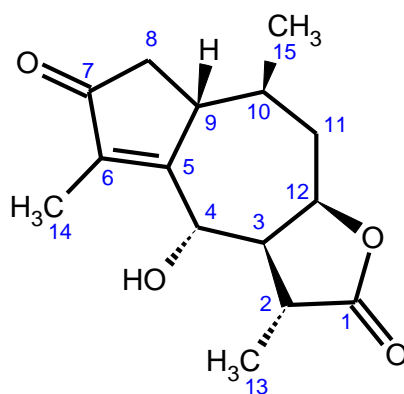


Figure 3.2: Geigerin

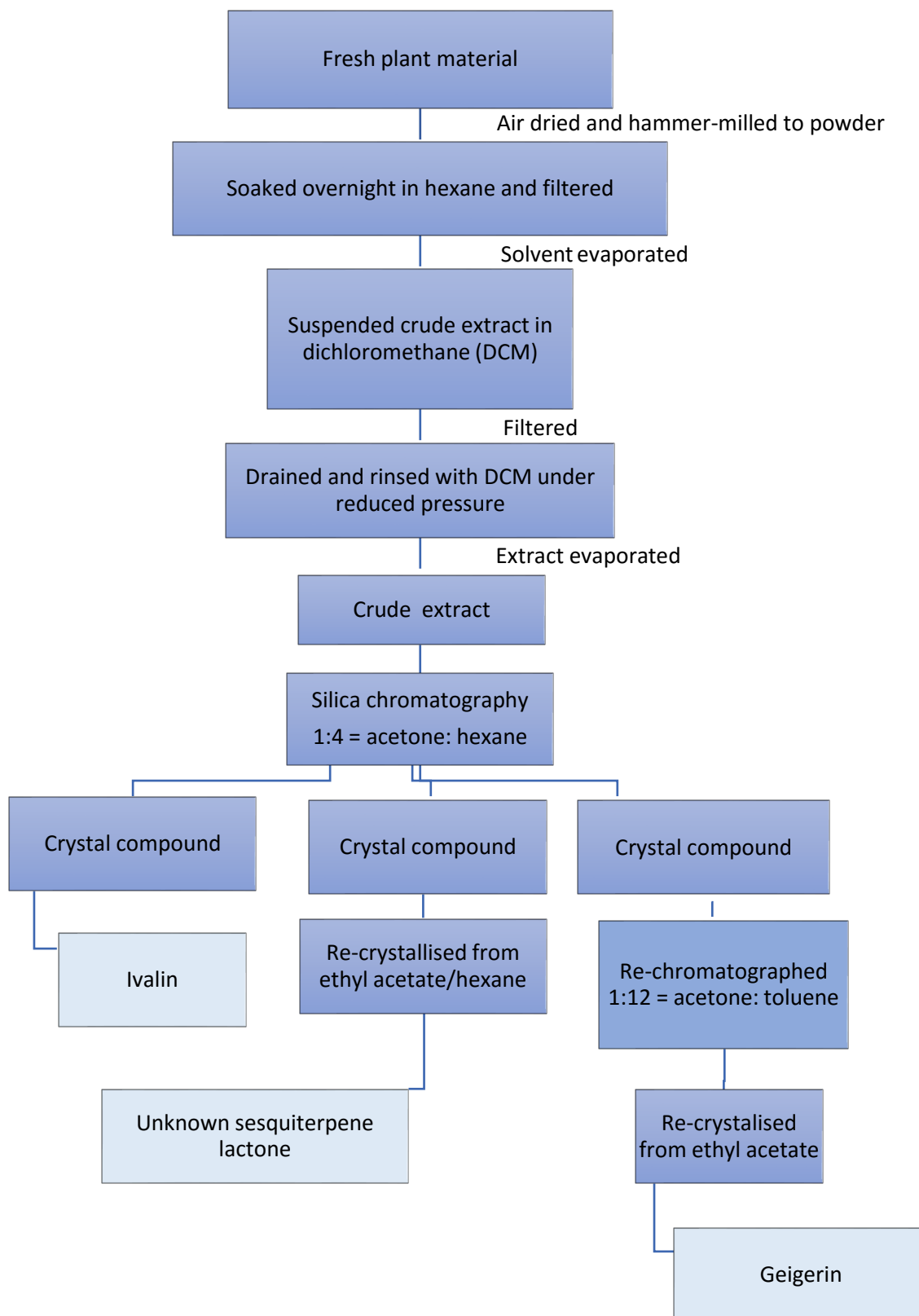


Figure 3.3: Schematic diagram of the extraction and isolation of ivalin, geigerin and the unknown sesquiterpene lactone.

3.1.2 Unknown sesquiterpene lactone identification

Structure elucidation of the unknown compound was performed with the assistance and under the guidance of Dr Fouché, an organic chemist, using nuclear magnetic resonance (NMR) and mass spectrometry. Absolute configuration was determined using X-ray crystal diffraction analyses. The compound's mass was analysed using positive ion high-resolution electrospray ionisation mass spectrometry (HRESIMS).

3.1.3 Parthenolide

Parthenolide (Figure 3.4), a commercially available sesquiterpene lactone, was purchased from Sigma-Aldrich (Darmstadt, Germany). Parthenolide has a chemical formula of $C_{15}H_{20}O_3$ and molar mass of 248.317 g/mol. It is isolated and purified from the feverfew plant, *Tanacetum parthenium*. The highest parthenolide concentrations occur in the flowers and fruit.

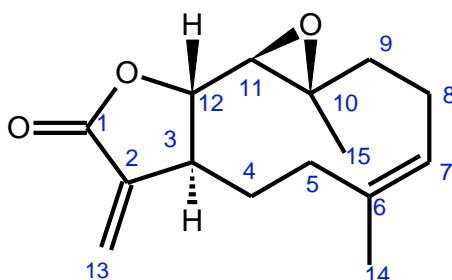


Figure 3.4: Parthenolide

3.2 Cell cultures

3.2.1 Chemicals, reagents and plastic ware

All chemicals, reagents and cell culture media were sourced from Sigma-Aldrich, Darmstadt, Germany, unless otherwise stated. Dulbecco's Modified Eagle's Medium (DMEM) was obtained from Pan Biotech (Aidenbach, Germany), foetal bovine serum (FBS) from Gibco (Thermo Fischer Scientific, Waltham, Massachusetts, USA), L-glutamine and penicillin/streptomycin from Lonza (Basel, Switzerland). Cell culture flasks and microplates

were acquired from Nunc, Roskilde, Denmark. Phosphate buffer, diethyl ether, acetonitrile, DMSO and acetone were purchased from Merck (Darmstadt, Germany).

3.2.2 Cell lines

Mouse skeletal myoblast (C2C12 [CRL-1772TM]) and rat embryonic cardiac myocyte (H9c2 (2-1) [CRL-1446TM]) cells were purchased from the American Tissue Culture Collection (ATCC; Manassas, Virginia, USA). The cells were cultured at 37°C in a humidified atmosphere of 5% CO₂ in high-glucose DMEM supplemented with 4 mM L-glutamine, 1 mM sodium pyruvate, 5% foetal calf serum (FCS) as well as 100 U/ml penicillin and 100 U/ml streptomycin (complete medium). After reaching 70-80% confluency, within 3-4 days, the medium was removed and the flasks rinsed twice with calcium and magnesium free phosphate buffered saline (PBS) at pH 7.4. Cells were detached from the flasks with 2 ml trypsin (0.25%)-ethylenediaminetetraacetic acid (EDTA) mixture and 1 ml for 75 cm² and 25 cm² flasks, respectively, at 37°C for 5 min. The trypsinisation was stopped by the addition of 13 and 9 ml of complete medium to the 75 cm² and 25 cm² flasks, respectively, before pelleting the cells by centrifugation at 130 x g for 7 min at room temperature. The cell pellet was re-suspended in 2 ml complete medium. The rapid trypan blue dye exclusion test based on the exclusion of the dye by viable cells with intact membranes was used to differentiate between viable (clear cytoplasm) and non-viable (blue stained cytoplasm) cells (Strober, 1997). Fifteen µl of this cell suspension was diluted 1:1 with 0.4% trypan blue dye solution in PBS and applied to a haemocytometer counting chamber (Neubauer-improved, Hirschmann, Eberstadt, Germany). A differential count of viable and non-viable cells was performed with the aid of a 20x microscope objective. The number of viable and non-viable cells in the cell suspension was calculated according to Equation 1.

$$\text{Cells/ml} = \frac{\text{Cells counted} \times \text{dilution factor} \times 10\,000}{\# \text{ of } 1 \text{ mm}^2 \text{ Squares}}$$

Equation 1: Calculation of cell number using a haemocytometer.

Experiments were performed with cells from stock cultures with different passage numbers and cell viability calculated using Equation 2. Viable cells from a stock culture were only used

if the viability exceeded 95% to ensure that cells from healthy cultures were used for cytotoxicity studies and to improve reproducibility between experiments.

$$\% \text{ viable cells} = \frac{(abs_{sample} - abs_{blank})}{(abs_{control} - abs_{blank})} \times 100$$

Equation 2: Calculation of percentage cell viability (blank: incubation medium, control: cells incubated in medium).

C2C12 cells from passage no. 5-15 and H9c2 cells from passage no. 17-27 were trypsinised, centrifuged and re-suspended in the incubation medium. Stock cultures were sub-cultured twice a week at 70-80% confluency to prevent differentiation of the myoblasts into myotubules, which may be initiated by a high cell confluency. To ensure reproducibility between experiments performed with cells from different cell passages, a constant splitting ratio was used to maintain the cells in the log growth phase for the duration of the experiment.

3.3 Exposure studies

C2C12 cells were seeded in a 96-well microplate at 1 500 cells/well and H9c2 cells at 10 000 cells/well, respectively, and allowed to attach for 24 h in a cell culture incubator (HeraCell 150, Thermo Scientific) at 37°C. After pre-incubation, the incubation medium was removed. The *Geigeria* toxins were solubilised in acetone and parthenolide in DMSO, followed by serial dilution in complete incubation medium supplemented with 5% FCS. The cells were exposed to 200 µl of a concentration range of ivalin, isogeigerin, geigerin and parthenolide, respectively for 24, 48 and 72 h. A positive control of doxorubicin (100 µM) was used (Green and Leeuwenburgh, 2002). Due to limited availability of isogeigerin acetate the cells were only exposed for 48 h to this toxin. During exposure the cells were maintained under controlled conditions to optimise their growth and viability. Exposure studies were performed in triplicate and repeated at least four times.

3.4 Cytotoxicity assay

3.4.1. MTT cytotoxicity assay

At completion of the exposure period the incubation medium was aspirated from the control and treated wells, followed by rinsing with 200 μ l PBS. The MTT assay was then performed by the addition of 200 μ l of DMEM and 20 μ l of water soluble MTT (5 mg/ml in PBS) to each well and the incubation continued for 2 h in the dark (plate covered with aluminium foil). After the medium was discarded, the insoluble dark purple formazan crystals, indicative of viable cells were solubilised by the addition of 100 μ l DMSO per well. The plates were covered with aluminium foil and lightly shaken on a 96-well plate shaker (Microporous, QB901, Newby) for 5 min. Viable cells were then quantified in terms of the intensity of the ABS of the solubilised formazan, read at 570 nm with a reference wavelength of 630 nm using a microplate reader (HT Synergy, Biotek).

3.5 Parthenolide metabolism

Due to insufficient quantities of the sesquiterpene lactones isolated from *Geigeria aspera*, it was decided to conduct the *in vitro* microsomal metabolism studies with the commercially available sesquiterpene lactone, parthenolide.

3.5.1 Liver microsomes

A commercially available mouse (CD-1, male) liver microsomal extract, rich in cytochrome P450 metabolic enzymes, was obtained from Sigma-Aldrich (Darmstadt, Germany). A method, primarily based on the method provided by Sigma-Aldrich, was optimised to evaluate the microsomal metabolism of parthenolide. Care was taken to maintain the metabolic activity of the microsomes stored at -80°C by gradual thawing on ice. The 200 μ l incubation volume consisted of 6 μ l of 20 mM NADPH dissolved in 100 mM of phosphate buffer (pH 7.4 at 37°C – sterile filtered and stored for a maximum period of 2 weeks at 4°C), 191 μ l of parthenolide (stock solution in DMSO solvent diluted in phosphate buffer to final concentration) and 3 μ l microsomes. Volumes of 3 μ l of thawed microsomes and 191 μ l parthenolide in phosphate buffer were mixed in a 1.5 ml Eppendorf tube. These were pre-incubated for 5 min in an orbital shaking incubator (MRC TU-400) at 39°C , before the microsomal enzymatic reaction was initiated by the addition of 6 μ l of the enzymatic co-factor, 20 mM NADPH.

After an incubation period of 60 min at 39°C in a shaking incubator, the reaction was quenched with the addition of 600 µl diethyl ether. The solution was vortexed for 2 min to ensure adequate extraction of the toxin and potential metabolites in the organic phase and then centrifuged at 4°C for 5 min at a speed of 10 000 x *g* (Allegra X22R Beckman centrifuge). The organic supernatant was transferred into a separate glass tube and evaporated at 40°C in a nitrogen evaporator (TurboVap LV, Zymark).

3.5.2 High performance liquid chromatography (HPLC)

Chromatographic analysis was performed on the Beckman Coulter System Gold comprising of a 168 Detector coupled to a UV source (Beckman, California, United States). The dried extract was solubilised in 200 µl mobile phase that consisted of acetonitrile:water (55:45) and injected at room temperature (21°C) into the HPLC at a solvent flow rate of 1ml/min, wavelength of 210 nm and a run time of 11 min. A BDS Hypersil C₁₈ column was used, equipped with 4 x 3 mm ID security guard cartridge and a column particle size of 5 µm (all from Phenomenex, Torrance CA, USA). An isocratic method was used.

3.6 Statistical analysis

The percentage cytotoxicity obtained from applying different concentrations of a toxic sesquiterpene lactone is a typical dose-response experiment and requires the fitting of the best model to represent the response. This was done for each time period separately (24, 48 and 72 h) for the two different cell lines. A logistic model is the best and most widely accepted model to fit if the data follows a typical sigmoidal (S-shape) trend and for calculation of the estimated median effective concentration (EC₅₀) (Motulsky, 2004). A logistic curve was fitted for ivalin and parthenolide cytotoxicity data in C2C12 cells using the model,

$$Y = A + C / (1 + \text{EXP}[-B * (X - M)]),$$

where X was the different (log₁₀) concentrations applied per toxin and cell line. The estimated regression parameter A is the minimum % toxicity, A + C is the maximum % toxicity, M is the EC₅₀ and B the maximum increase in toxicity at EC₅₀. For data following an exponential trend; i.e. the ivalin and parthenolide toxicity data in H9c2 cells, geigerin cytotoxicity in C2C12 cells and 48 h isogeigerin toxicity data in both cell lines; the ordinary exponential curve, also known as the asymptotic regression curve, was fitted. The model,

$$Y = A + B \times (R)^X$$

represents a curve rising from an asymptote and was fitted to the different (\log_{10}) concentrations (X) applied per toxin and cell line. The estimated regression parameter A is the minimum % toxicity, R determines the shape of the curve and B is the rate of increase. The EC_{50} was calculated from this model. Thereafter the test of parallelism was applied to ascertain if the curves differed between times for the same cell line and at the same time between different cell lines. If most curves were exponential then the estimated regression parameters (not times) were compared as exponential curves, otherwise as logistic curves (Payne, 2017).

Accumulated analysis of variance (ANOVA) was used to statistically interpret the overall logistic fit between Y (% toxicity) and X (logarithmic [\log_{10}] concentration of toxin) for all exposure times as well as differences between exposure time at the lowest toxin concentrations, the highest toxin concentrations and the slope of the dose-response curve at the EC_{50} . Data were analysed using the statistical program GenStat® (VSN International, 2017).

Chapter 4: Results

4.1 Identification, spectrometry and stereochemical characterization of the unknown compound

4.1.1 Identity of unknown compound

From the spectroscopic data, the colourless, crystalline, unknown sesquiterpene lactone was identified as isogeigerin acetate (Figure 4.1).

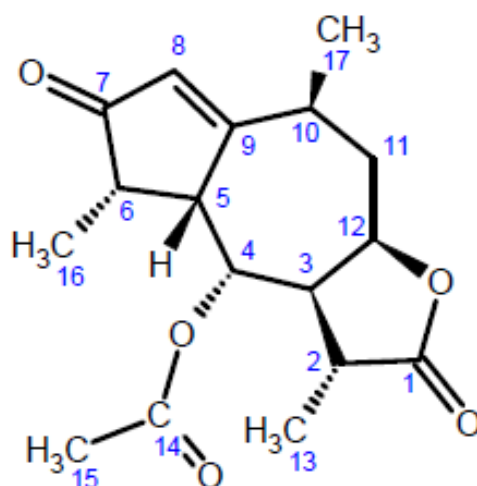


Figure 4.1: Isogeigerin acetate.

4.1.2 Mass spectrometry

A mass spectrum of isogeigerin acetate is presented in Figure 4.2. The chemical formula is $C_{17}H_{22}O_5$ with a molecular weight of 306.34 g/mol. The HRESIMS data revealed a pseudo-molecular ion at m/z 307.1519 (calculated for $C_{17}H_{23}O_5$ $[M+H]^+$) and a fragment peak at m/z 247.1337 $[-HOAc]$ due to the loss of an acetate group.

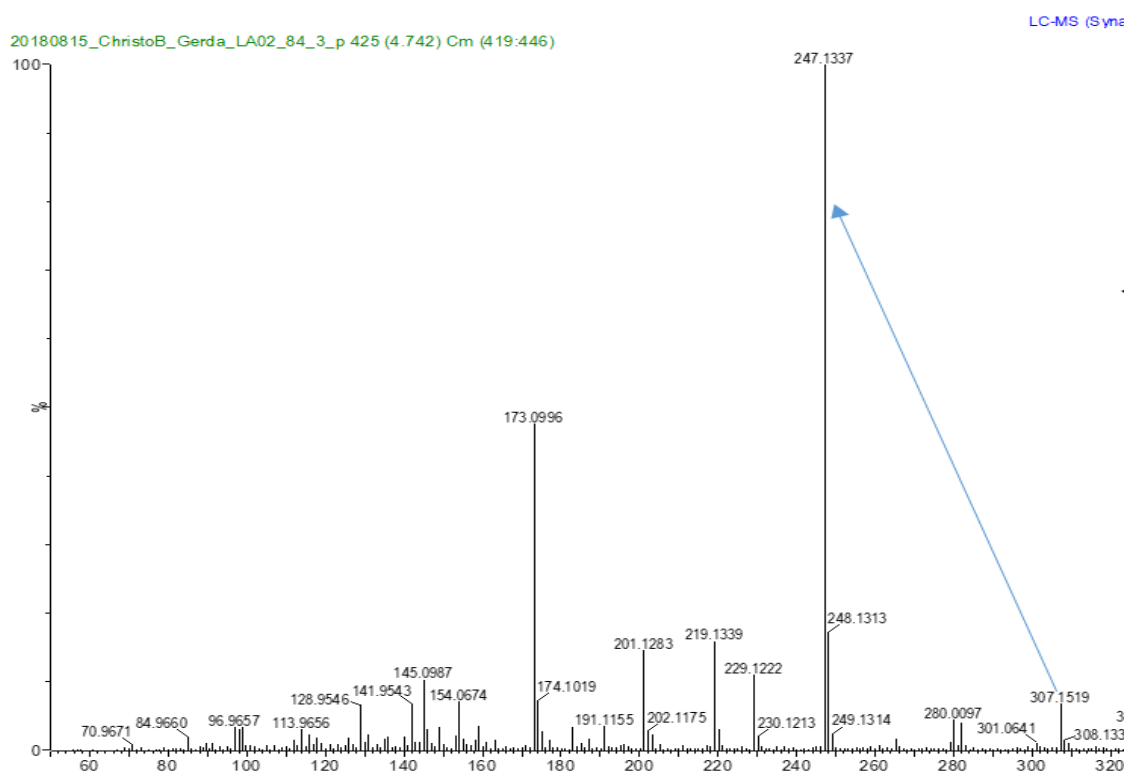


Figure 4.2: The ESI TOF mass spectrum of isogeigerin acetate.

4.1.3 NMR spectrum

The ^1H NMR spectrum of isogeigerin acetate displayed three methyl doublets, no methylene signal was observed, but the presence of an acetyl group was suggested. The ^1H and ^{13}C NMR data are summarised in Table 4.1.

Table 4.1. NMR spectroscopic data for isogeigerin acetate.

Carbon Position	Carbon type	$\delta_{\text{C}}/\text{ppm}$	$\delta_{\text{H}}/\text{ppm}$ (J in Hz)
1	-C=O	176.9	-
2	-CH	34.9	2.51 (dq, 1H)
3	-CH	48.8	2.65 (dddd, 1H, $J = 3.1; 3.1; 3.1; 3.1$)
4	-CH	68.5	5.20 (brd, 1H, $J = 3.1$)
5	-CH	42.6	3.38 (brd, 1H, $J = 6.5$)
6	-CH	44.1	2.57 (m, 1H)
7	-C=O	209.2	-
8	-CH	130.2	6.05 (brt, 1H)
9	-C	181.1	-
10	-CH	31.4	2.76 (m, 1H)
11	-CH ₂	36.2	1.90 (m, 2H)
12	-CH	79.0	4.56 (m, 1H)
13	-CH ₃	22.1	1.30 (d, 3H, $J = 6.6$)
14	-OCO	169.6	-
15	-OCOCH ₃	21.2	1.92 (s, 3H)
16	-CH ₃	11.1	0.98 (d, 3H, $J = 7.9$)
17	-CH ₃	13.3	1.32 (d, 3H, $J = 6.6$)

4.1.4 X-ray analysis

The structure and absolute stereochemistry of isogeigerin acetate (Figure 4.3) was confirmed by X-ray crystallographic analysis to be: (3R,3aR,4R,4aR,5S,8S,9aR)-3,5,8-trimethyl-2,6-dioxo-2,3,3a,4,4a,5,6,8,9,9a-decahydro-azuleno[6,5-b]furan-4-yl acetate. The crystal was colourless and the X-ray intensity dimensions measured were 0.168 mm x 0.201 mm x 0.248 mm.

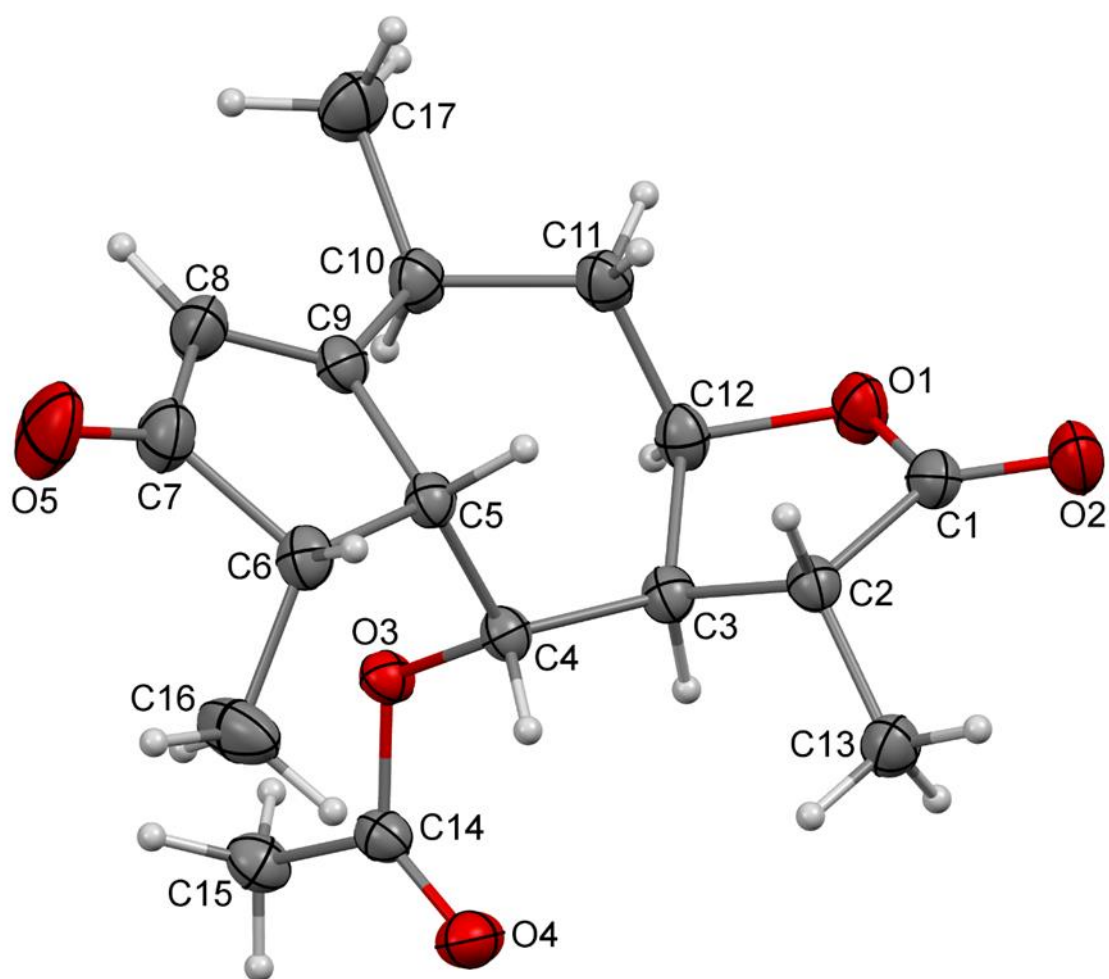


Figure 4.3: *MERCURY* drawing of the structure of isogeigerin acetate showing the stereochemistry of the molecule (Fouché *et al.*, 2019).

4.2. *In vitro* cytotoxicity of sesquiterpene lactones - ivalin, isogeigerin acetate, geigerin and parthenolide - in C2C12 and H9c2 cell lines

4.2.1 Cytotoxic effect of ivalin, isogeigerin acetate, geigerin and parthenolide

Semi-logarithmic concentration response plots of C2C12 myoblasts exposed to ivalin (Figure 4.4) showed that the logistic curves fitted at 48 and 72 h were similar, but differed from the 24 h curve as indicated by the slope of the curve and EC_{50} parameters. The overall logistic fit between percentage toxicity (Y) and log concentration of ivalin (X) was highly significant ($p < 0.001$) for all the different exposure times. The minimum percentage toxicities of the curves differed significantly ($p = 0.039$), whilst no significant difference ($p = 0.124$) in the maximum percentage toxicities was observed. The EC_{50} 's were $2.7 (\pm 1.593) \mu\text{M}$ at 24 h; $2.973 (\pm 1.188) \mu\text{M}$ at 48 h and $3.313 (\pm 1.205) \mu\text{M}$ at 72 h. The slopes of the curves differed significantly ($p = 0.014$) between the incubation times. The difference was more pronounced at concentrations above the EC_{50} . A concentration-dependent cytotoxic response of ivalin was observed.

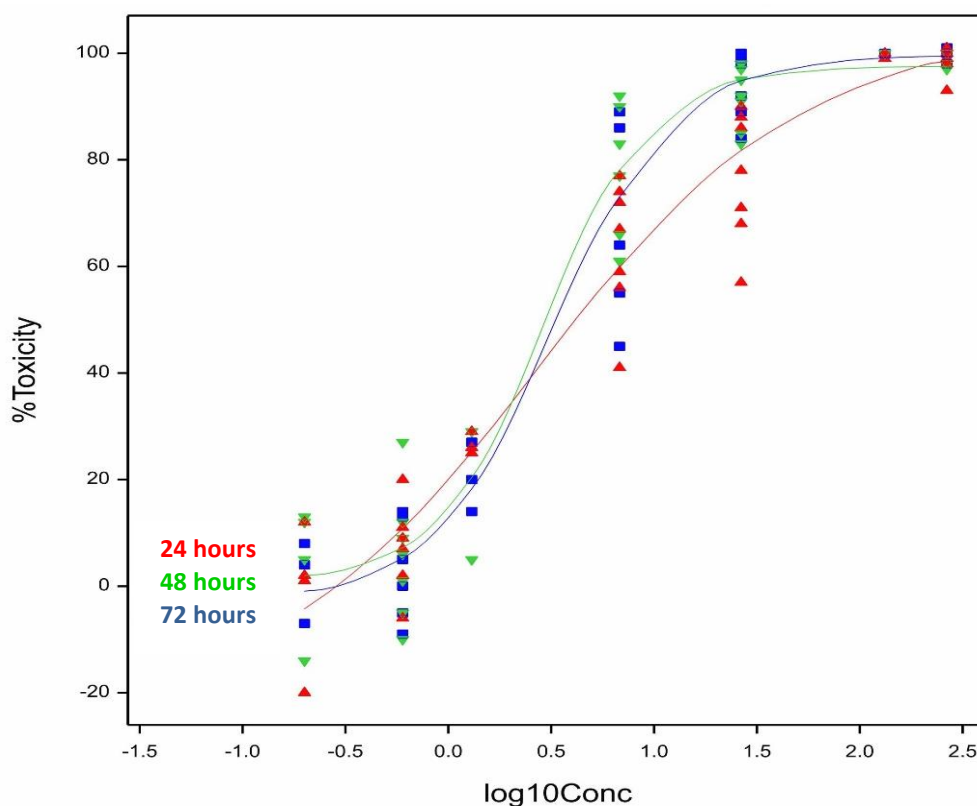


Figure 4.4: Logistic curves of the observed and fitted relationship following exposure of C2C12 myoblasts to ivalin (μM) for 24, 48 and 72 h.

The cytotoxic effect of isogeigerin acetate on C2C12 and H9c2 cells after 48 h exposure was plotted as an exponential curve (Figure 4.5). The minimum % toxicity, the rate of increase and the shape of the curves differed significantly ($p < 0.001$) between the cell lines. An EC_{50} of 3877 (± 1.063) μM was calculated for the C2C12 myoblasts and an extrapolated EC_{50} of 9977 (± 1.150) μM was estimated for the H9c2 cells.

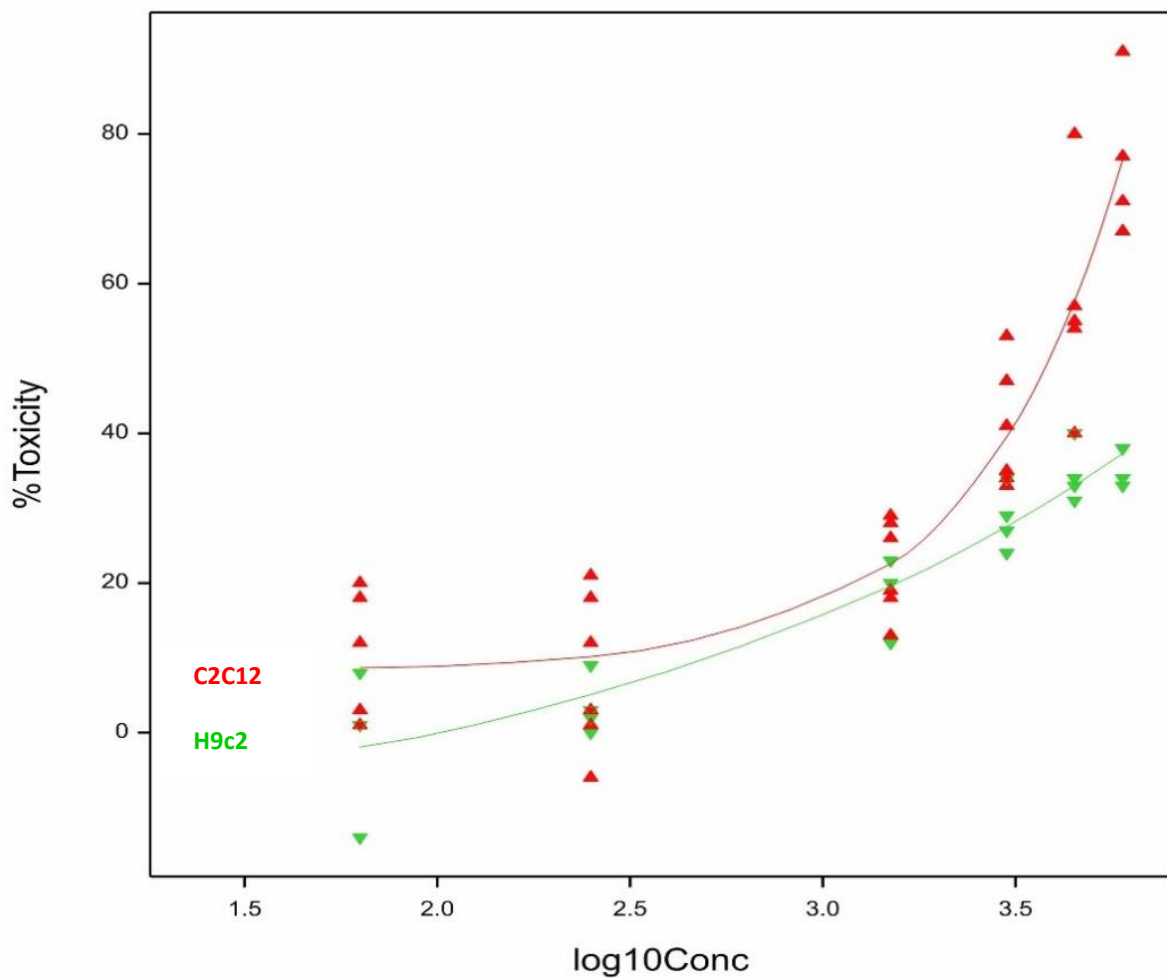


Figure 4.5: Exponential curves of the observed and fitted relationship following exposure of C2C12 myoblasts and H9c2 cardiac myocytes to isogeigerin acetate (μM) for 48 h.

The exponential curves of cytotoxicity in C2C12 cells exposed to geigerin revealed that the fitted curves at 48 and 72 h were very similar and differed from the curve at 24 h as indicated by the rate of increase (Figure 4.6). The fit between the percentage toxicity and log concentration of geigerin was highly significant ($p < 0.001$), whilst the minimum percentage toxicity ($p = 0.002$) and rate of increase ($p < 0.001$) also differed significantly. However, there was no significant difference ($p = 0.774$) in the slope of the curves between the three exposure times.

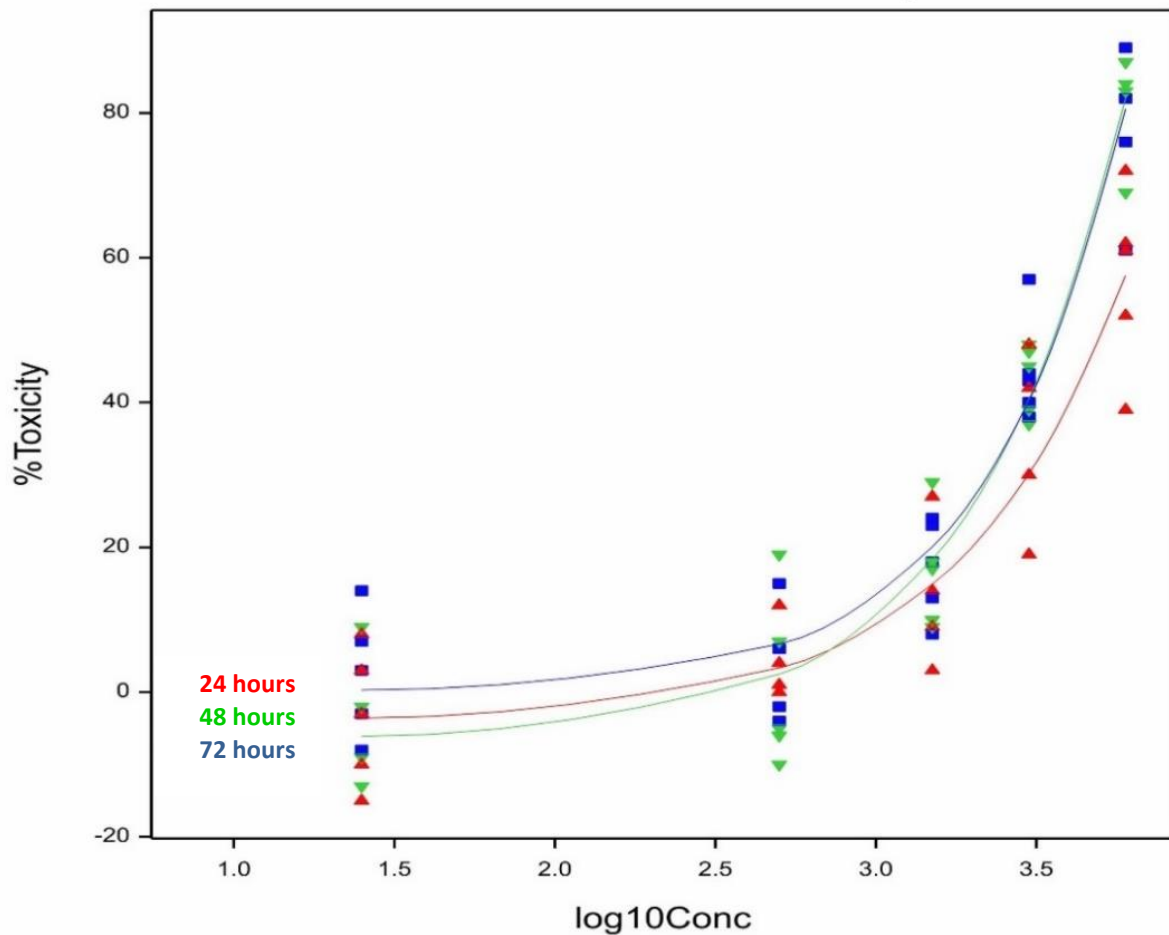


Figure 4.6: Exponential curves of the observed and fitted relationship following exposure of C2C12 myoblasts to geigerin (μM) for 24, 48 and 72 h.

The exposure of C2C12 cells to parthenolide showed that the logistic fit (Figure 4.7) between the percentage toxicity and log concentration was highly significant ($p < 0.001$). However, none of the other parameters; the slope, minimum and maximum toxicities; differed significantly ($p > 0.05$) at all the exposure times. The half maximal effective concentrations (EC_{50} 's) of parthenolide were similar after 48 ($4.779 \pm 1.137 \mu\text{M}$) and 72 h ($4.708 \pm 1.066 \mu\text{M}$). At 24 h the EC_{50} was determined to be $5.595 (\pm 1.220) \mu\text{M}$.

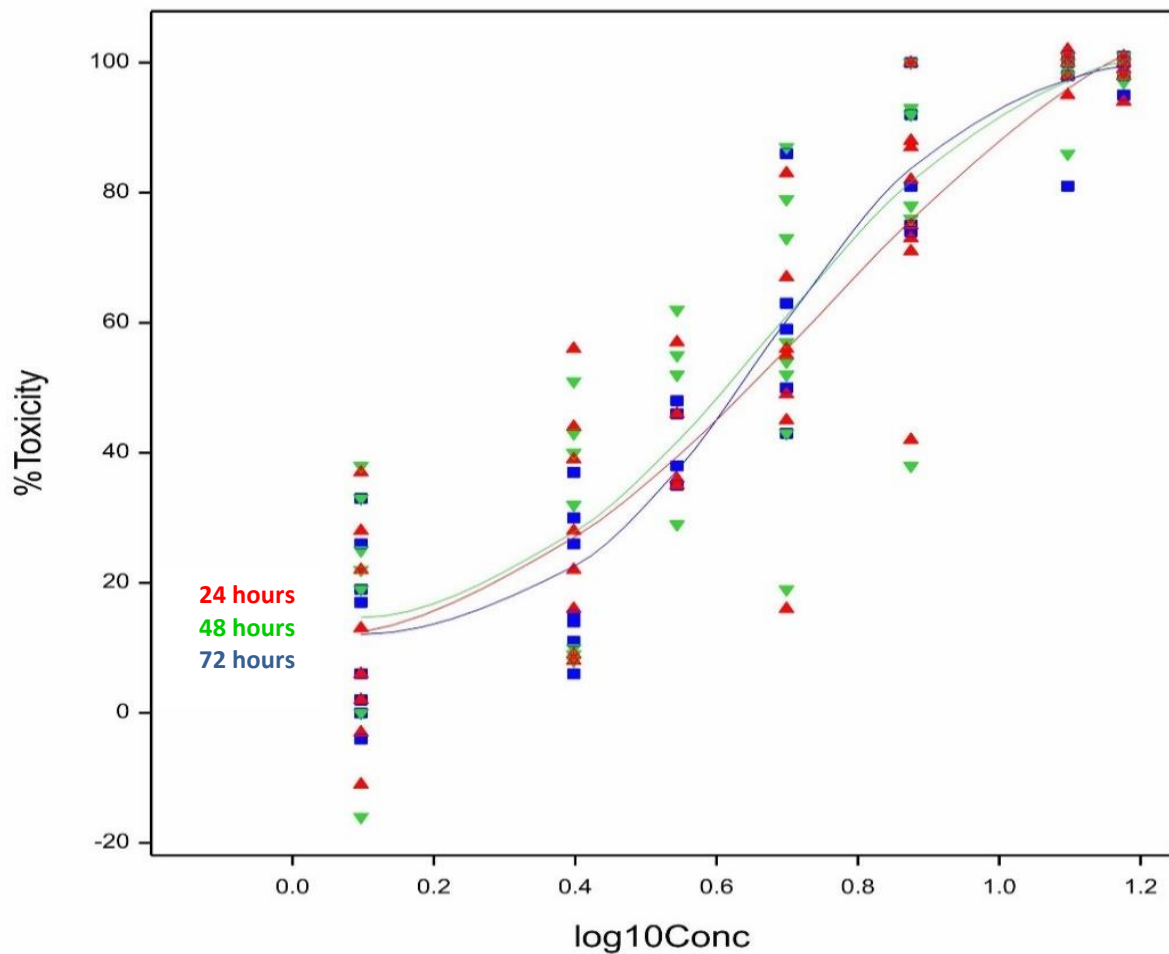


Figure 4.7: Logistic curves of the observed and fitted relationship following exposure of C2C12 myoblasts to parthenolide (μM) for 24, 48 and 72 h.

4.2.2 Cytotoxic effect of ivalin and parthenolide on H9c2 cells.

The exponential curves of ivalin fitted at 24, 48 and 72 h showed a highly significant difference ($p < 0.05$) in terms of the minimum percentage toxicity and the shape of the curves, but not in terms of the rate of increase ($p > 0.05$). Therefore, the form and shape of the curves were significantly different ($p < 0.05$) as can be seen from the graph (Figure 4.8). The EC_{50} 's of ivalin after 24 h was $60.65 (\pm 1.106) \mu\text{M}$, after 48 h it was $17.79 (\pm 1.128) \mu\text{M}$ and 72 h it was $8.448 (\pm 1.287) \mu\text{M}$. A concentration-dependent cytotoxic response was observed.

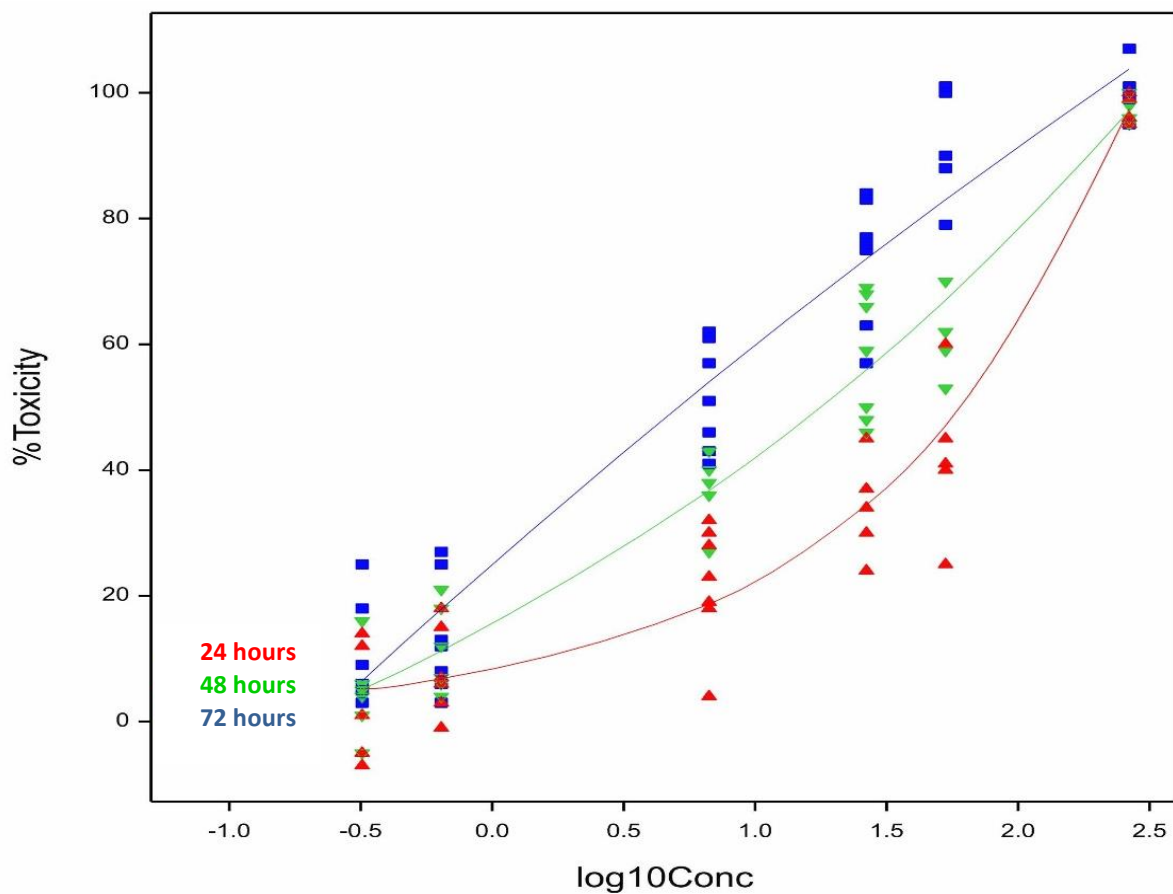


Figure 4.8: Exponential curves of the observed and fitted relationship following exposure of H9c2 cardiac myocytes to ivalin (μM) for 24, 48 and 72 h.

The three curves of parthenolide fitted at 24, 48 and 72 h differed significantly ($p < 0.05$) in terms of the minimum percentage toxicity, but not in rate of increase ($p > 0.05$) and shape of the curves ($p > 0.05$) (Figure 4.9). Therefore, the form and shape of the curves were not significantly different as can be seen from the graph. The EC_{50} 's observed after exposure were $20.8 (\pm 1.020) \mu\text{M}$ after 24 h; $18.40 (\pm 1.028) \mu\text{M}$ after 48 h and $17.40 (\pm 1.039) \mu\text{M}$ after 72 h, respectively. At exposure times 48 and 72 h, the curves were most similar. Cytotoxicity of parthenolide increased in a dose-dependent manner.

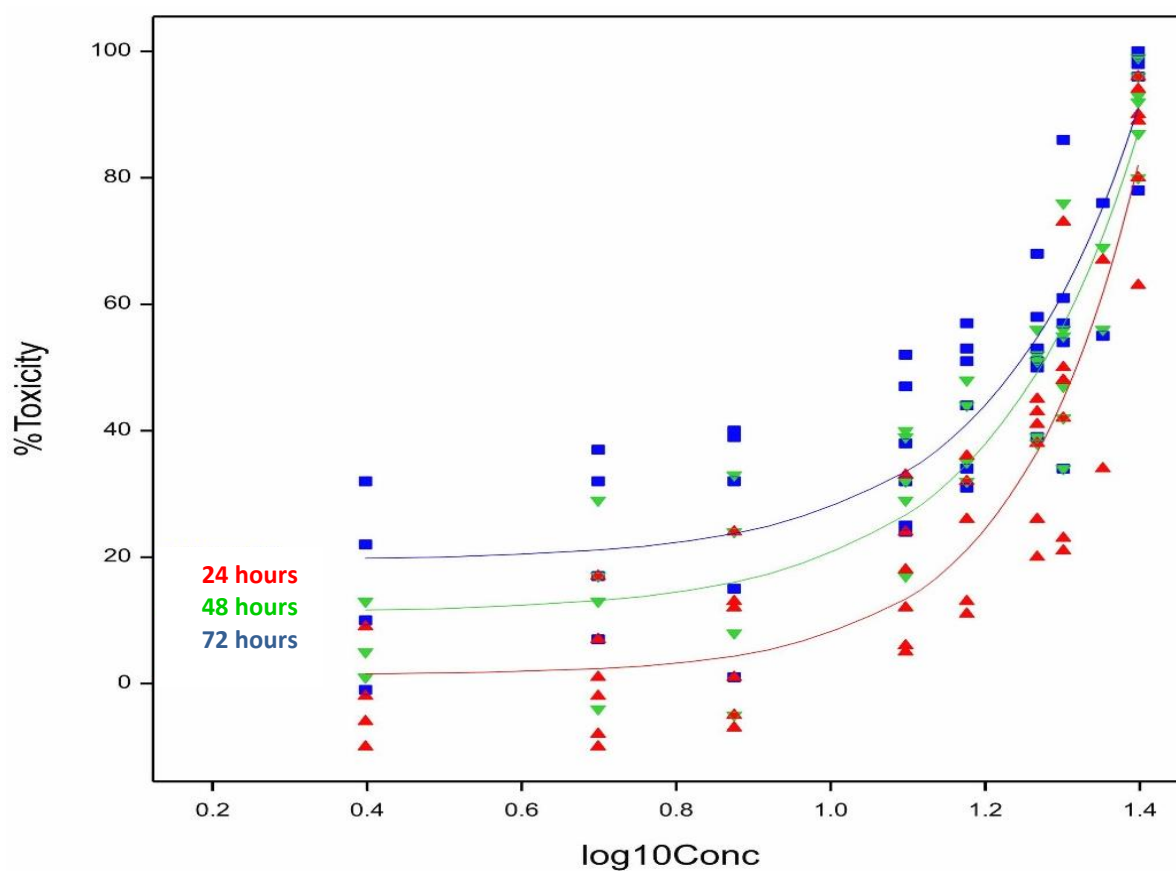


Figure 4.9: Exponential curves of the observed and fitted relationship following exposure of H9c2 cardiac myocytes to parthenolide (μM) for 24, 48 and 72h.

The sesquiterpene lactones exhibited different toxic effects in C2C12 and H9c2 cells in a concentration-dependent manner. The EC₅₀'s (μM) and standard errors of the means of the EC₅₀'s for the experimental repeats of the sesquiterpene lactones tested on both cell lines are presented in Table 4.2.

Table 4.2: EC₅₀'s of ivalin, isogeigerin acetate, geigerin and parthenolide determined on C2C12 and H9c2 cells after 24, 48 and 72 h exposure times.

Cell Lines	Exposure time (h)	Sesquiterpene lactones EC ₅₀ s (μM)			
		Ivalin	Isogeigerin acetate	Geigerin	Parthenolide
C2C12	24	2.7 ± 1.593 n = 7	–	5141 ± 1.075 n = 5	5.595 ± 1.220 n = 8
	48	2.973 ± 1.188 n = 7	3877 ± 1.063 n = 6	3673 ± 1.051 n = 5	4.779 ± 1.137 n = 8
	72	3.313 ± 1.205 n = 7	–	3727 ± 1.059 n = 5	4.708 ± 1.066 n = 8
H9c2	24	60.65 ± 1.106 n = 7	–	–	20.8 ± 1.020 n = 6
	48	17.79 ± 1.128 n = 7	9977 ± 1.150 n = 4	–	18.40 ± 1.028 n = 6
	72	8.448 ± 1.287 n = 7	–	–	17.40 ± 1.039 n = 6

EC₅₀ (μM) ± Standard error of the mean (SE) for at least 4 experimental repeats (n).

4.3 In vitro hepatic microsomal metabolism of parthenolide determined by HPLC

A sensitive and selective HPLC method was established. Parthenolide was detected and after incubation with a commercially acquired male mouse liver microsomal fraction, a metabolite was present. The separation of the compounds was dependent on their polarity and resulted in different retention times. The retention times of the background peaks of the microsomal incubation buffer, excluding the microsomal fraction and parthenolide, are depicted in the chromatogram (Figure 4.10).

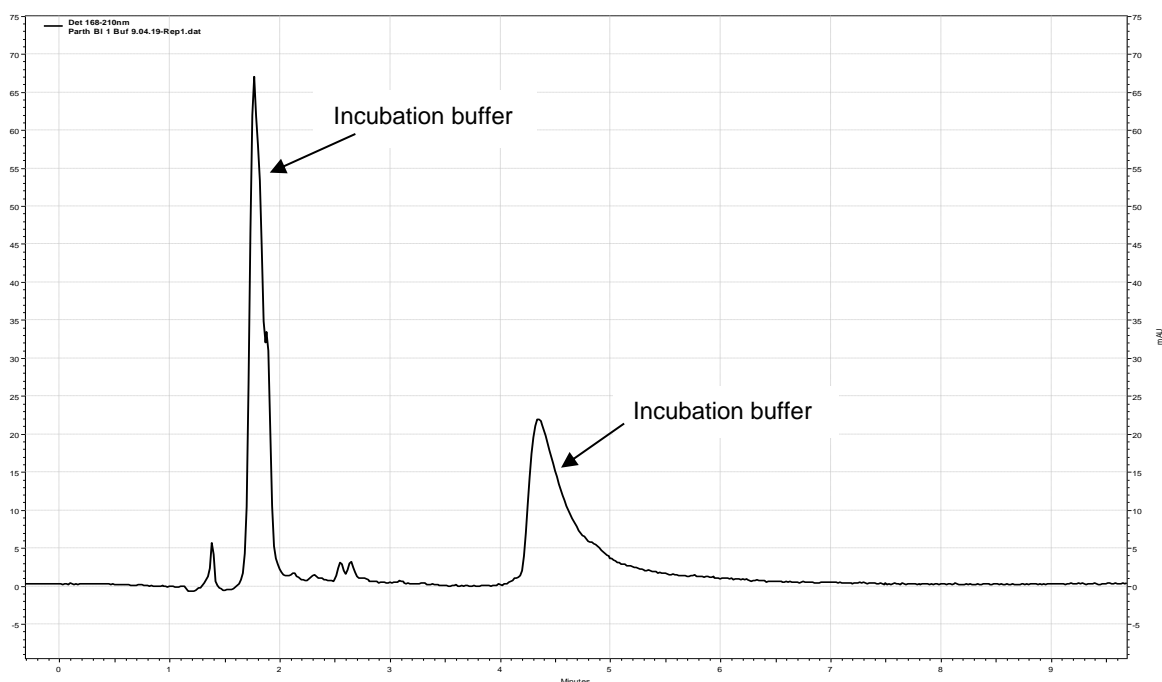


Figure 4.10: HPLC chromatogram, only incubation buffer (blank).

As shown in Figure 4.11, a microsomal peak appeared at a retention time of 2.7 min, when the microsomal fraction (without parthenolide) was incubated in the buffer.

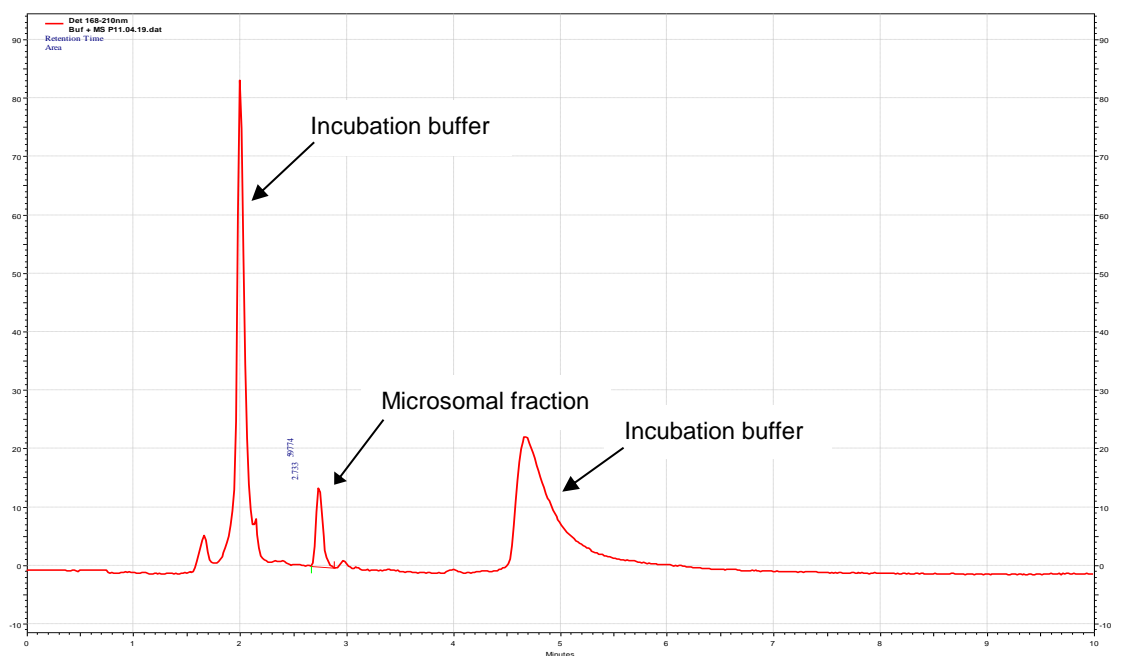


Figure 4.11: HPLC chromatogram of only the microsomal fraction incubated in the buffer.

Parthenolide was analysed, without and with a fixed concentration of the microsomal fraction, over a concentration range of 4.25 to 53 μM (Figures 4.12 - 4.16). The increasing trend in the height and area of the parthenolide peaks corresponded with the increase in the parthenolide concentrations. When increasing concentrations of parthenolide was incubated with the microsomal fraction, the chromatograms indicate the metabolism of parthenolide in the presence of the Phase I CYP450 enzymes contained by the microsomal fraction. Parthenolide and the resultant metabolite peaks were observed at retention times 6.5 min and 3.8 min, respectively. Well defined peaks of the eluted compounds were observed with no interfering peaks.

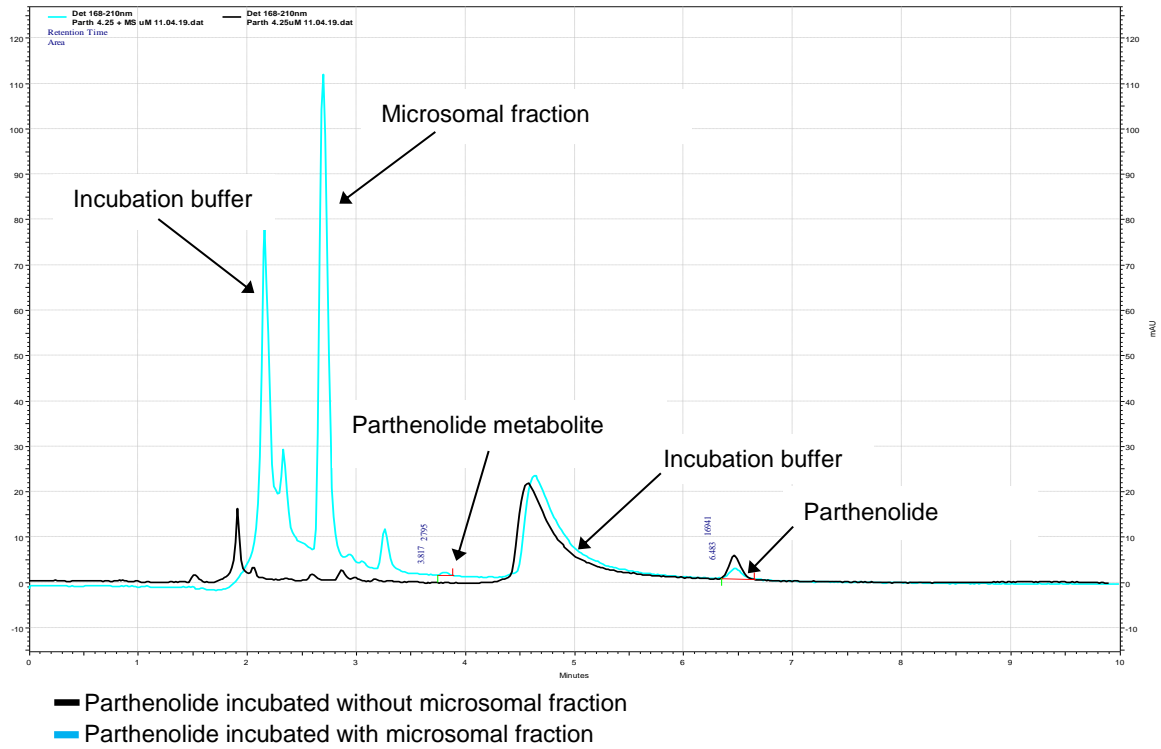


Figure 4.12: Parthenolide (4.25 μM) incubated without and with microsomal fraction.

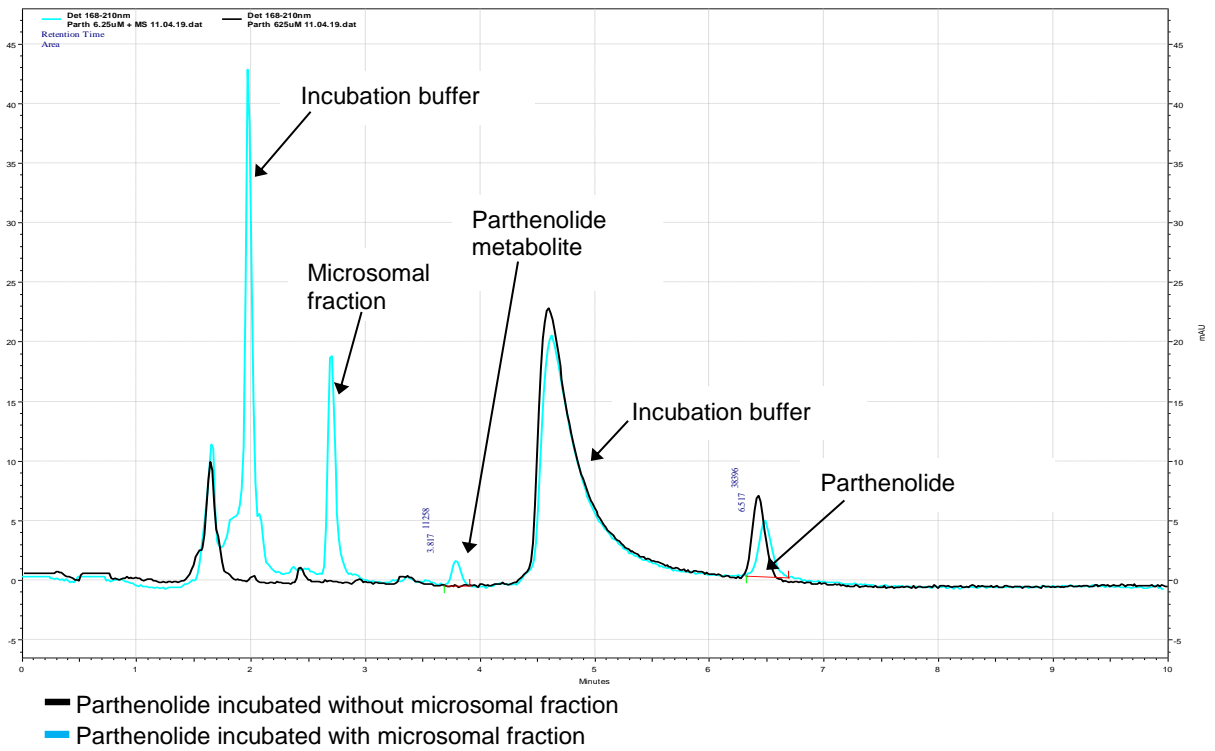


Figure 4.13: Parthenolide (6.25 μM) incubated without and with microsomal fraction.

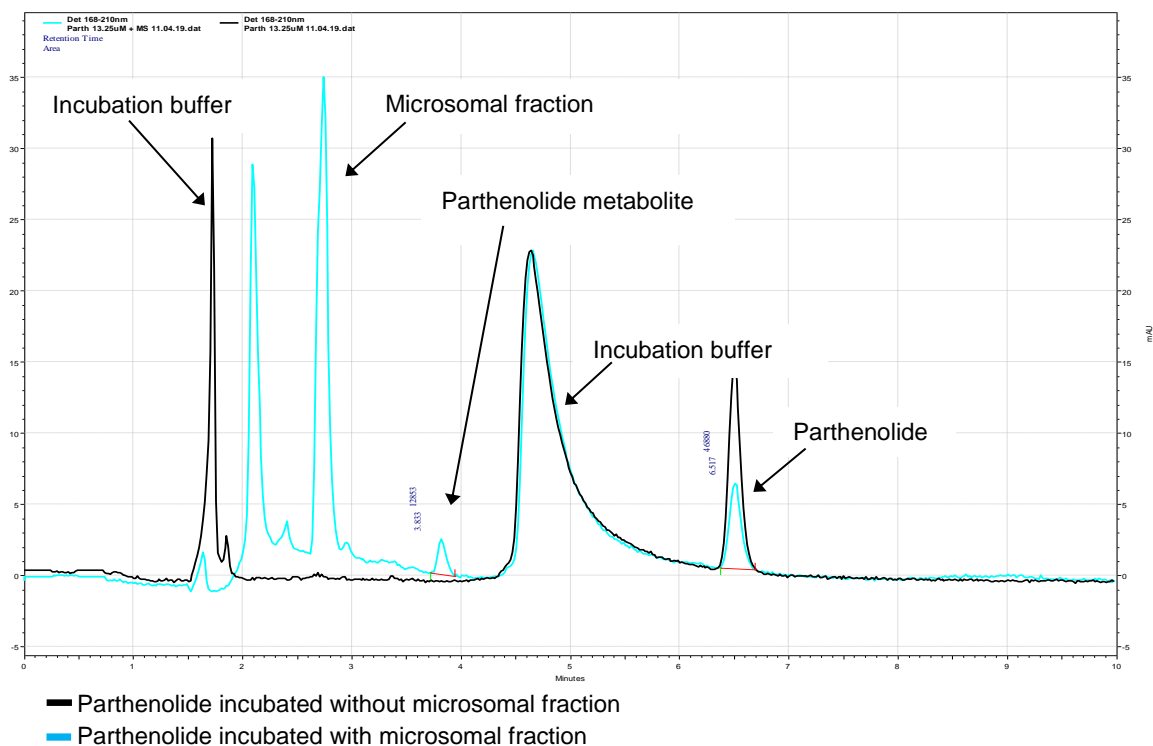


Figure 4.14: Parthenolide (13.25 μM) incubated without and with microsomal fraction.

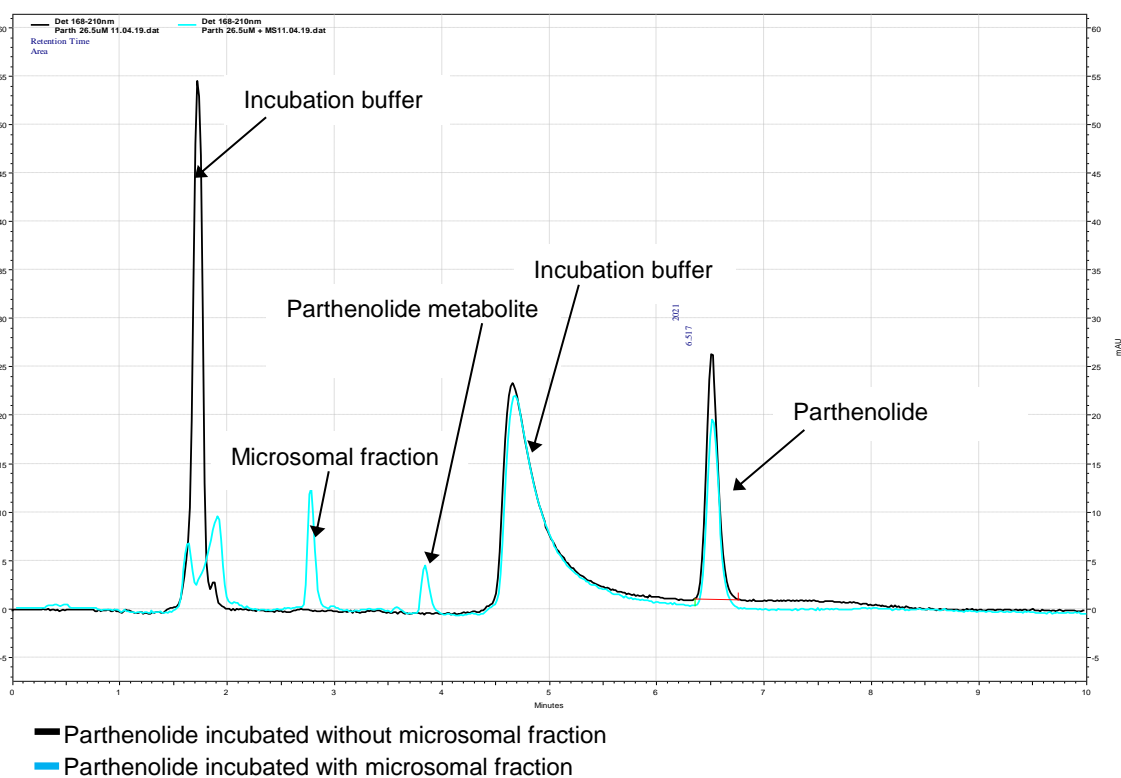


Figure 4.15: Parthenolide (26.5 μM) incubated without and with microsomal fraction.

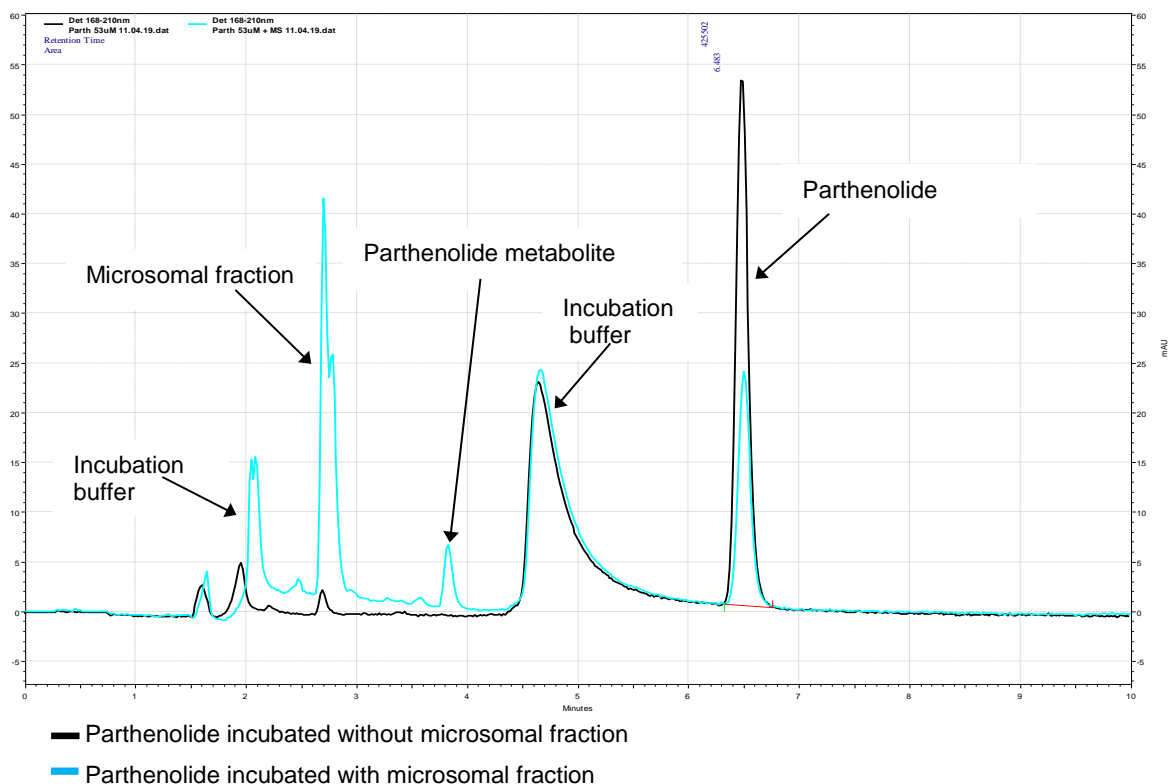


Figure 4.16: Parthenolide (53 µM) incubated without and with microsomal fraction.

Figure 4.17 is the overlay of all the individual chromatograms following incubation of increasing concentrations of parthenolide with the microsomal fraction. After incubation with the microsomal fraction there was a decrease in the peak height (Figures 12-16) and area of parthenolide (Figure 4.18). At least one metabolite was discerned. A concomitant increase in this metabolite peak area was observed, which correlated with increasing concentrations of parthenolide added (Table 4.3 and Figure 4.18). The yield of the metabolite depended on the concentration of parthenolide incubated in the presence of microsomal enzymes. A plot of the parthenolide (without and with microsomal incubation) and metabolite peak areas illustrated the linear relationship (Figure 4.19). The strength of the positive linear association was corroborated by excellent R^2 values (Figure 4.19).

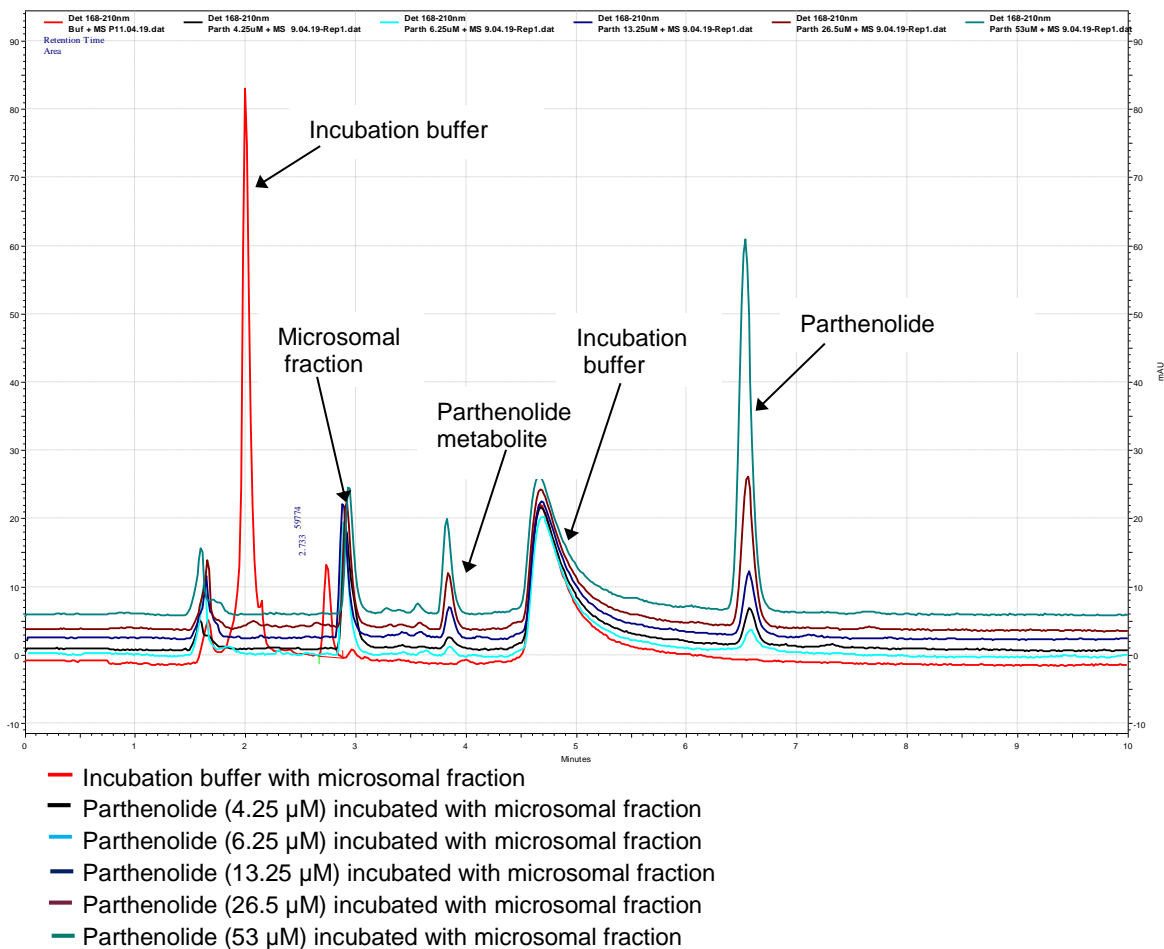


Figure 4.17: Overlay of HPLC chromatograms of parthenolide incubated at increasing concentrations (4.25, 6.625, 13.25, 26.5 and 53 μM) with the microsomal fraction.

Table 4.3: Parthenolide incubated without and with microsomal fraction.

Parthenolide (μM)	Parthenolide peak area (-) microsomes	Parthenolide peak area (+) microsomes	Parthenolide retention time (min)	Metabolite area	Metabolite retention time (min)
4.25	36 805	18 952	6.567	6 516	3.850
6.625	56 013	25 891	6.517	9 501	3.817
13.25	107 658	60 724	6.517	19 087	3.833
26.5	222 238	169 750	6.550	35 907	3.833
53	473 849	373 133	6.667	68 962	3.867

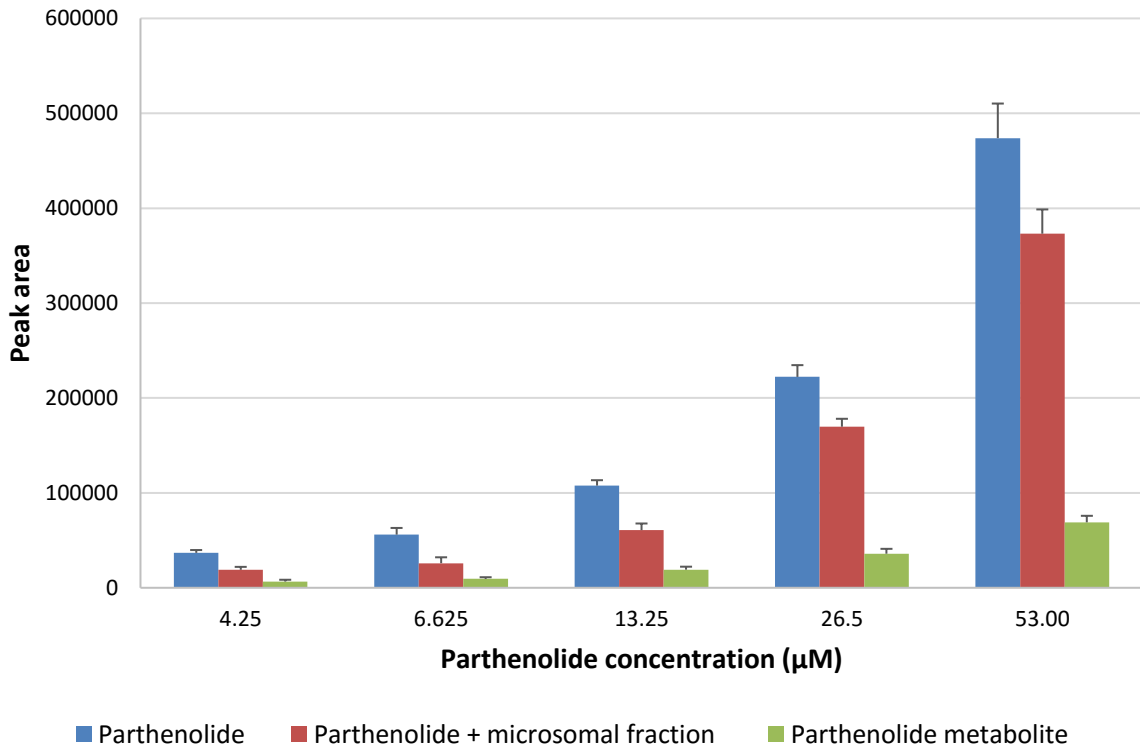


Figure 4.18: Metabolism of parthenolide after incubation with the microsomal fraction as detected by HPLC.

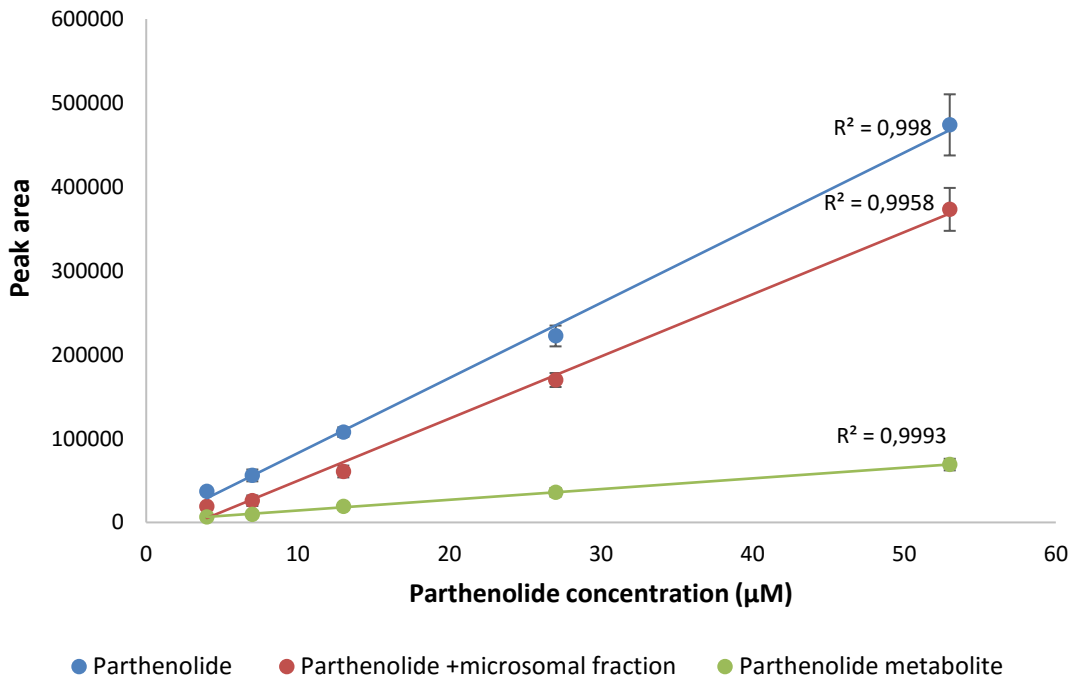


Figure 4.19: Linear relationship of parthenolide at increasing concentrations, incubated without and with the microsomal fraction, and the metabolite as detected by HPLC.

Chapter 5: Discussion

The plant poisoning vermeersiekte also referred to as “vomiting disease” affects ruminants, mainly sheep, after ingestion of sufficient quantities of *Geigeria* plant material containing the active compounds, i.e. sesquiterpene lactones. When the disease could not be induced in a sheep after dosing with an isolated sesquiterpene lactone, geigerin (Rimington and Roets, 1936), over two days, it was realised that the disease was induced as result of a cumulative effect or exposure to a mixture of sesquiterpene lactones ingested over time (Kellerman, 2005). The sesquiterpene lactones, geigerin and ivalin, thoroughly described in literature (Grosskopf, 1964; Kellerman *et al.*, 2005) and an “unknown” sesquiterpene lactone, later identified as isogeigerin acetate, were isolated and purified in the departmental laboratory from *Geigeria aspera*, the most toxic of the *Geigeria* species.

The structure of isogeigerin acetate was elucidated using spectroscopic techniques, 1 and 2D, ¹H- and ¹³C-NMR spectroscopy and mass spectrometry. A literature search confirmed that this compound had previously been isolated and the stereochemistry was partially defined by Bohlman *et al.* (1982). The absolute stereochemistry of isogeigerin acetate was deduced by using X-ray crystallographic analysis (Fouché *et al.*, 2019). The X-ray crystallographic data of isogeigerin acetate showed that its structure is similar to geigerin. The differences between geigerin and isogeigerin acetate occur at the ring double bond in geigerin between C-5 and C-6 that shifted to between C-8 and C-9 in isogeigerin acetate. Furthermore, the hydroxyl group bonded to C-4 in geigerin, had been esterified to form an acetate in isogeigerin acetate.

To study the *in vitro* cytotoxicity of the abovementioned compounds at cellular level, mouse skeletal myoblasts (C2C12) and rat embryonic cardiac myocytes (H9c2), representing the skeletal, cardiac and oesophageal muscles affected in sheep, after ingestion of *Geigeria* plant material, were employed. Botha *et al.* (2017) concluded that the mouse myoblast C2C12 cells were a suitable *in vitro* model to study the cytotoxicity of geigerin and possibly other sesquiterpene lactones.

Parthenolide, a commercially available sesquiterpene lactone isolated and purified from the feverfew, *Tanacetum parthenium* (Seca *et al.*, 2017), was included in the current study as standard. The cytotoxicity of parthenolide on rat H9c2 cardiomyocytes was previously

evaluated by Tsai *et al.* (2015). After exposing H9c2 cells for 15 h to different concentrations (0–100 μM) of parthenolide, and using the MTT-assay, a concentration-dependent cell death was observed (Tsai *et al.*, 2015).

In the current study, concentration and time-dependent cytotoxic effects in terms of basal cellular viability, using the MTT viability assay, were evaluated for 48 h for isogeigerin acetate and for 24, 48 and 72 h for the other sesquiterpene lactones tested. The viability of the cells was monitored in relation to the negative control (cells in complete medium). A positive mitochondrial control, doxorubicin (100 μM), resulting in a 100% toxic effect, was included as a quality control for the MTT assay (Green and Leeuwenburgh, 2002). Sesquiterpene lactones are known inhibitors of mitochondrial respiration (Van Aswegen *et al.*, 1979; Van Aswegen *et al.*, 1982; Tsai *et al.*, 2015) and thus the MTT assay, monitoring mitochondrial activity, is a sensitive tool to study the cytotoxic effect of sesquiterpene lactones *in vitro*. The cell density used in the cytotoxicity studies was determined by the cell inoculum required to maintain a log growth phase for the duration of the 72 h exposure period and the working range of the MTT assay; i.e. a linear relationship must be maintained between the absorbance intensity measured and the amount of formazan formed indicative of the number of viable cells (Da Silva Gasque *et al.*, 2014; Mossman, 1983). In preliminary studies, it was ascertained that C2C12 cells had a higher growth rate than H9c2 cells. Thus, a much lower initial cell inoculum, 1 500 C2C12 cells compared to 10 000 H9c2 cells were required to maintain the cells in the log growth phase for maximum duration of the study (72 h).

The curves fitted to depict the relationship between cytotoxicity and concentration; i.e. logistic for ivalin (Figure 4.4) and parthenolide in C2C12 cells (Figure 4.7); and exponential for geigerin in C2C12 cells (Figure 4.6), ivalin (Figure 4.8) and parthenolide in H9c2 cells (Figure 4.9) and isogeigerin acetate in both cell lines (Figures 4.5), were highly significant indicating that the best models were chosen to reflect the biological dose-response. The relationship between the cytotoxicity induced in C2C12 cells and toxin concentration for ivalin and parthenolide displayed the typical biological dose-response sigmoidal curve. Exposure concentrations for this study was selected to ensure that the cytotoxic effects spanned the 50% effect (lower and higher concentrations) to ensure the accurate estimation of the EC_{50} . The cytotoxic effects ranged from $\leq 15\%$ for the minimum effect to 99% for the maximum effect. However, for H9c2 cells exposed to isogeigerin the maximum cytotoxic effect achieved

was only 46% (Figure 4.5). Limited quantities of isogeigerin was available, which did not allow the concentration to be increased further to obtain a 50% effect and both C2C12 and H9c2 cells lines were only exposed to isogeigerin acetate for 48 h.

The statistical difference of the cytotoxic effects at the lowest concentrations tested between incubations time within cell lines were significant for ivalin ($p=0.039$) and geigerin ($p=0.002$) in C2C12 cells (Figures 4.4 and 4.6); and ivalin ($p<0.05$) and parthenolide ($p<0.05$) in H9c2 cells (Figures 4.8 and 4.9), showing that there is a positive relationship between exposure time and cytotoxicity caused at low concentrations. The cytotoxic dose-response plot of ivalin in C2C12 cells (Figure 4. 4) showed that there was a significant difference ($p=0.014$) in the slope of the curves, thus indicating cytotoxic effect between all three exposure times, but the 48 and 72 h exposure curves were more steep and the difference was more pronounced at concentrations above the EC_{50} . However, the cytotoxic effect of parthenolide on C2C12 cells (Figure 4.7) was not affected by exposure time, as no significant differences ($p>0.05$) in any of the logistic plot parameters (minimum and maximum toxicity) were observed. This is also evidenced by the similar parthenolide EC_{50} 's of 5.59, 4.78 and 4.71 μM , after 24, 48 and 72 h, respectively (Table 4.2).

No significant differences ($p>0.05$) were evident in the shape of the exponential curves for geigerin exposure in C2C12 cells (Figure 4.6) and parthenolide exposure in H9c2 cells (Figure 4.9). Nevertheless, the rate of increase in geigerin-induced toxicity with increase in exposure concentration (Figure 4.6) did differ significantly ($p<0.001$) indicating that exposure time contributed positively to the toxic effect at a given concentration.

The plot of the cytotoxicity of ivalin in H9c2 cells (Figure 4.8) showed that there was a significant difference ($p<0.05$) in the shape of the curves and from that one would expect that there would be a significant difference in increase of toxicity between different concentrations at the different exposure times, but to the contrary the difference in rate of increase of toxic effect was not significant ($p>0.05$). This probably could be ascribed to the variation in the biological repeats.

The trends of plots of parthenolide exposure in H9c2 cells (Figure 4.9) look similar and this observation was supported by the fact that the rate of increase in cytotoxicity and the shape of the curves did not differ significantly ($p>0.05$). The significant difference ($p<0.05$) between

exposure time and toxic effect at the lowest concentration noted before, therefore diminished with increase in concentration.

When comparing the EC₅₀'s of all the sesquiterpene lactones tested in both cell lines (Table 4.2), the EC₅₀'s of ivalin and parthenolide were similar, with concentrations in the μM range, whereas the EC₅₀'s of geigerin and isogeigerin acetate were a 1000 times higher, at concentrations in the mM range. When comparing the EC₅₀'s of ivalin and parthenolide exposure of C2C12 cells, it appears that ivalin is slightly more toxic. The sensitivity of H9c2 cells following ivalin exposure increased with an increase in exposure time. The increase in sensitivity between 24 and 72 h was 7 times, indicating that exposure time played a major role in the susceptibility of H9c2 cells to ivalin when compared to C2C12. The same comparison for parthenolide cannot be made, because the EC₅₀'s for parthenolide, within both cell lines and for different exposure times, did not change meaningfully. The differences between exposure times for sesquiterpene lactones within cell lines and between cell lines were statistically evaluated, but because of limitations of the statistical approaches used the difference in cytotoxic effects between different sesquiterpene lactones within and between cell lines could not be compared.

The EC₅₀ (Table 4.2) estimated for geigerin for C2C12 cells after 24 h exposure; i.e. 5141 μM compared well with the 5000 μM resulting in a 50.4% cytotoxic effect reported by Botha *et al.* (2017), notwithstanding the fact that the cell density used was 13x more compared to the current study. The EC₅₀ of 20.8 μM determined for parthenolide in H9c2 cells after 24 h exposure in this study, compared well with a cytotoxic effect of about 65% reported by Tsai *et al.* (2015) after 15 h exposure to 30 μM parthenolide, even though they used 1.5x more H9c2 cells, in their study.

The EC₅₀'s estimated for the sesquiterpene lactones after different exposure times (Table 4.2) show that in the case of C2C12 cells, ivalin is the most toxic (EC₅₀'s for 24, 48 and 72 h of 2.7 ± 1.593; 2.973 ± 1.88 and 3.313 ± 1.205 μM, respectively). Ivalin was also the only sesquiterpene lactone tested in C2C12 cells for which EC₅₀ values increased slightly with increasing incubation times. This phenomenon was also described in a study where literature was reviewed to investigate the role of incubation time in *in vitro* cytotoxicity testing using primary human hepatocytes (Gu *et al.*, 2018). Thus, it appears that C2C12 cells become more

resistant to ivalin with increasing exposure times. As the same effect was not observed with H9c2 cells, the effect cannot be ascribed to a decrease in solubility of ivalin at higher concentrations and longer exposure times.

In C2C12 cells, parthenolide was the second most toxic sesquiterpene lactone (EC_{50} 's, for 24, 48 and 72 h of 5.595 ± 1.220 ; 4.779 ± 1.137 and 4.708 ± 1.066 μM , respectively). The cytotoxicity induced by geigerin (EC_{50} 's for 24, 48 and 72 h of 5141 ± 1.075 ; 3673 ± 1.051 and 3727 ± 1.059 μM , respectively) and isogeigerin acetate (EC_{50} at 48 h of 3877 ± 1.063 μM) in C2C12 cells were more or less the same.

However, in H9c2 cells parthenolide (EC_{50} of 20.8 ± 1.020 μM) after 24 h exposure was more toxic than ivalin (EC_{50} of 60.65 ± 1.106 μM). There was no noteworthy difference in the cytotoxicities of parthenolide (EC_{50} 's, for 24, 48 and 72 h of 20.8 ± 1.020 ; 18.40 ± 1.028 and 17.40 ± 1.039 μM , respectively) in H9c2 cells with increasing exposure time, whilst the toxicity of ivalin (EC_{50} 's for 24, 48 and 72 h of 60.65 ± 1.106 ; 17.79 ± 1.128 and 8.448 ± 1.287 μM , respectively) in H9c2 cells increased with increasing exposure time and at 72 h it was more toxic than parthenolide (Table 4.2). Similar to C2C12 cells, isogeigerin acetate (EC_{50} of 9977 ± 1.150 , after 48 h) was also much less toxic in H9c2 cells compared to ivalin and parthenolide. In both C2C12 and H9c2 cells exposure time affected cytotoxicity of ivalin, whilst no major differences in cytotoxicity induced by parthenolide were noticed. Exposure time also did not play a role in the cytotoxicity of geigerin in C2C12 cells (Table 4.2).

When comparing the effect of increasing incubation time on EC_{50} 's of all the sesquiterpene lactones tested, the decrease of the EC_{50} of ivalin in H9c2 cells is much more pronounced than for the other sesquiterpene lactones tested (Table 4.2). Vermeesiekte results after repetitive ingestion of *Geigeria* plant material and, thus, there is a cumulative dose effect *in vivo* (Botha *et al.*, 2017; Kellerman *et al.*, 2005). It seems that a cumulative effect over time plays an important role in cytotoxicity of ivalin in H9c2 cells.

The lower EC_{50} 's (Table 4.2) estimated for ivalin and parthenolide indicated that they were more toxic than isogeigerin acetate and geigerin. The enhanced sensitivity of both cell lines to ivalin and parthenolide at low micromolar concentrations compared to geigerin and isogeigerin at low millimolar concentrations can according to Rodriguez *et al.* (1976) be ascribed to the presence of an α -methylene- γ -lactone group present in both sesquiterpene

lactones at C-2. This α -methylene- γ -lactone group interferes with the action of enzymes by alkylation of nucleophile groups in their structure changing the chemical structure and stereospecificity of their active sites (Gaspar *et al.*, 1987). Ivalin also has a second exocyclic methylene (CH₂) group at C-6 (Figure 3.1). Furthermore, the addition of an extra exomethylene on the lactone appears to enhance the toxicities of these sesquiterpene lactones even further (Picman *et al.*, 1986; Rodriguez *et al.*, 1976). Ivalin was 1 000 times more toxic than isogeigerin acetate and geigerin in the C2C12 cells and 500 times more toxic than isogeigerin acetate in H9c2 cells. Isogeigerin acetate and geigerin, the least toxic, both lack the exocyclic-methylene group. High concentrations of geigerin and isogeigerin acetate were required to induce cytotoxicity. This observation is corroborated by the *in vitro* study conducted by Botha *et al.* (2017) where high geigerin concentrations (2 – 5 mM) were required to induce cytotoxicity in the C2C12 cell line, which was ascribed to the cumulative effect of sesquiterpene lactones associated with vermeersiekte.

To explain the difference in cytotoxicity between the C2C12 and H9c2 cells for the individual sesquiterpene lactones tested the following limitations must be considered; i.e. species differences, the difference in number of mitochondria in muscle cells from organs with a different metabolic activity and different cell densities used in exposure studies. Caviglia *et al.* (2013) reported that the observed correlation between rate of cell death and initial cell density only applied to the lowest concentration in their study. They proposed that the higher rate of cell proliferation at a low cell density, because of more available space, will enhance the sensitivity of the cells (Caviglia *et al.*, 2013). However, in this study the faster growing C2C12 cells were seeded at a lower cell density to compensate for the difference in growth rates with H9c2 cells. Although the EC₅₀'s obtained for geigerin in C2C12 cells compared well with the cytotoxic effect elicited by a similar geigerin concentration at a different cell density by Botha *et al.* (2017), we cannot conclude that the difference in cell densities between the two cells lines studied, had an effect on the results.

Mitochondrial activity was used as a cytotoxicity endpoint in this study. The number of mitochondria, the producer of ATP in muscle, depends on muscle type and individual physical activity. Park *et al.* (2014) concluded that mitochondrial respiratory rates decreased progressively from cardiac- to skeletal- to smooth muscle. Mitochondrial density in skeletal muscle, as expressed as percentage of cardiac muscle, varies between 33-52% in humans

(Park *et al.*, 2014). In addition, mouse hearts, on average, beat 1.5 times faster than rat hearts (Papadimitriou *et al.*, 2008). However, when working with immortalised cell lines even from the same species, one must bear in mind that they were established from different animals; i.e. individual, sex and age variation will apply. Some immortalised cell lines have also retained more characteristics from primary cells compared to others; i.e. it was reported that the H9c2 rat cardiomyocytes (also used in this study) were more similar to primary cardiomyocytes regarding mitochondrial energy metabolism compared to a mouse cardiomyocyte cell line, HL-1 (Kuznetsova *et al.*, 2015). Thus, a more comprehensive study will be required before deductions can be made with respect to the effect of species *per se*, cell density and different muscle groups on cytotoxicity of sesquiterpene lactones *in vitro*.

In vivo, after *Geigeria* plant material is ingested, the active toxic principles will be absorbed and transported to the liver via the portal circulation where it can be biotransformed to metabolites, which can be more or less toxic. The combined effect of the sesquiterpene lactones and their potential biotransformed products on targeted cells was not evaluated in this study. However, to investigate the potential biotransformation of a sesquiterpene lactone by the liver and to optimise the monitoring of the biotransformation process, parthenolide was incubated with a mouse liver microsomal fraction, enriched for Phase I CYP450 enzymes and the possible biotransformation products assessed by HPLC. The incubation and HPLC conditions were optimised for parthenolide incubated without and with the microsomal fraction.

Figures 4.12 - 4.16 depict the reproducible chromatograms obtained when increasing concentrations of parthenolide, ranging from 4.25 – 53 μM , was incubated without and with a fixed concentration of the microsomal fraction. A steady increase in the peak heights can be observed. This is supported by the increase in peak areas as measured at each concentration (Table 4.3). Figure 4.17 is an overlay of all the chromatograms of increasing concentrations of parthenolide incubated with the microsomal fraction to demonstrate the relationship between the different concentrations tested. A stable increase in the metabolite peak heights was noticeable. The chromatograms of the incubation buffer (Figure 4.10) and microsomal fraction (Figure 4.11) showed a few unidentified peaks that might be ascribed to the salt content of the incubation buffer and the microsomal protein fractions that co-extracted with the parthenolide and parthenolide metabolites.

In the bar chart (Figure 4.18) and Table 4.3 it can be seen that the area under the parthenolide peak decreased following incubation with the microsomal enzymes and that the area under the metabolite peak increased accordingly. The linear relationships (Figure 4.19) between increasing parthenolide concentrations, parthenolide remaining after biotransformation and the metabolite formed, respectively, confirmed that the parthenolide incubation, extraction and HPLC conditions were optimised successfully. This also demonstrated that parthenolide can be biotransformed by the liver and that parthenolide can be accurately measured at the concentration range tested. Since the microsomal fraction is enriched for Phase I CYP450 metabolic enzymes (Timbrell, 2008), the biotransformation of parthenolide observed can only be ascribed to these enzymes and the effect of *in vivo* Phase II enzymatic biotransformations were not considered in this study. The linear relationship between parthenolide concentration and metabolite (Figure 4.19) showed that the reaction rate depended on substrate concentration and that the reaction thus followed first-order kinetics (Jia and Liu, 2007) at the concentration range studied.

Chapter 6: Conclusions

The structure of the unknown sesquiterpene lactone isolated from *Geigeria aspera*, the most toxic *Geigeria* species responsible for vermeersiekte in sheep, was clarified as isogeigerin acetate. The chemical structure of isogeigerin acetate was similar to geigerin, but the ring double bond between C-5 and C-6 in geigerin had shifted to between C-8 and C-9 and the hydroxyl group bonded to C-4 in geigerin had been esterified to form an acetate.

The cytotoxicity of the *Geigeria aspera* sesquiterpene lactones; namely isogeigerin acetate, geigerin and ivalin; and parthenolide from the feverfew plant, *Tanacetum parthenium*, used as standard, were evaluated on mouse skeletal myoblasts (C2C12) and rat embryonic cardiac myocytes (H9c2), representing the target cells from affected tissues of sheep that have contracted vermeersiekte. It was concluded that the chemical structure of the sesquiterpene lactones, especially the presence of an α -methylene- γ -lactone group in ivalin and parthenolide, contributed to the enhanced toxicity of these two sesquiterpene lactones as compared to isogeigerin acetate and geigerin. In general exposure time enhanced the cytotoxicity of the sesquiterpene lactones, except for the cytotoxic effect of ivalin on C2C12 cells, where the resistance of the cells increased with an increasing exposure time. The rat cardiomyocytes, H9c2 cells, were more resistant to the sesquiterpenes lactones than the C2C12 mouse skeletal myoblasts. Future research projects can also compare *in vitro* cytotoxicity where a combination of or different ratios of the toxic sesquiterpene lactones, isolated from vermeerbosies, are exposed to cell lines.

Incubation and HPLC conditions were also optimised to assess if parthenolide could be biotransformed, when incubated with a commercially available mouse liver microsomal fraction. At least one metabolite was detected. Future studies should investigate the metabolism of the sesquiterpene lactones contained by the various *Geigeria* species and establish if the metabolites are more or less toxic. The chemical structure of the metabolites produced should also be ascertained and the CYP450 isoenzyme(s), responsible for biotransformation, could be identified. The roles that biotransformation of these compounds by Phase I and Phase II liver enzymes play in their ultimate and interactive toxicity, must also still be determined.

The subcellular effects of these sesquiterpene lactones with respect to their interaction with cytoskeletal proteins and filaments are not clear at present and further studies are in progress to elucidate the possible mechanism of action of the sesquiterpene lactones associated with vermeersiekte. In addition, an effective treatment for exposed animals, targeting affected muscle groups at the cellular level must be identified, and hence the necessity to duplicate the interactions of the toxins and their metabolites *in vivo*.

Chapter 7: References

Ahmed, S.A., Gogal Jr, R.M. and Walsh, J.E., 1994. A new rapid and simple non-radioactive assay to monitor and determine the proliferation of lymphocytes: an alternative to [³H] thymidine incorporation assay. *Journal of Immunological Methods* 170(2), 211-224.

Aslantürk, Ö.S., 2018. *In Vitro* Cytotoxicity and Cell Viability Assays: *Principles, Advantages, and Disadvantages*. <http://dx.doi.org/10.5772/intechopen.71923>.

Bertoli, A., Ruffoni, B., Pistelli, L. and Pistelli, L., 2010. Analytical methods for the extraction and identification of secondary metabolite production in 'in vitro' plant cell cultures. In *Bio-farms for Nutraceuticals*, pp. 250-266, Springer, Boston, Massachusetts.

Bohlmann, B., Zdero, C. and Ahmed, M., 1982. New sesquiterpene lactones, geranylinalol derivatives and other constituents from *Geigeria species*. *Phytochemistry* 21(7), 1679-1691.

Botha, C.J., Clift, S.J., Ferreira, G.C. and Masango, M.G., 2017. Geigerin-induced cytotoxicity in a murine myoblast cell line (C2C12). *Onderstepoort Journal of Veterinary Research* 84(1), 1-7.

Botha, C.J., Gous, T.A., Penrith, M.L., Naudé, T.W., Labuschagne, L. and Retief, E., 1997. Vermeersiekte caused by *Geigeria burkei* Harv. subsp. *burkei* var. *hirtella* Merxm. in the Northern Province of South Africa: research communication. *Journal of the South African Veterinary Association* 68(3), 97-101.

Botha, C.J. and Venter, E., 2002. University of Pretoria. Faculty of Veterinary Science. Department of Paraclinical Sciences. Section Pharmacology and Toxicology, Uniform Resource identifier: <http://hdl.handle.net/2263/8539>.

Botha, C.J., Venter, E.A., Ferreira, G.C., Phaswane, R.M. and Clift, S.J., 2019. Geigerin-induced disorganization of desmin, an intermediate filament of the cytoskeleton, in a murine myoblast cell line (C2C12). *Toxicon* 167, 162-167.

Brandon, E.F.A., Raap, C.D., Meijerman, I., Beijnen, J.H. and Schellens, J.H.M., 2003. An update on *in vitro* test methods in human hepatic drug biotransformation research: pros and cons. *Toxicology and Applied Pharmacology* 189, 233-246.

Caviglia, C., Zór, K., Canepa, S., Carminati, M. Muhammad H.B., Raiteri, R. Andresen, T.L., Heiskanen A. and Emnéus, T. 2013. Interdependence of initial cell density, drug concentration and exposure time revealed by realtime impedance spectroscopic cytotoxicity assay. *Analyst* 00,1-7, DOI: [10.1039/x0xx00000x](https://doi.org/10.1039/x0xx00000x).

Chadwick, M., Trewin, H., Gawthrop, F. and Wagstaff, C., 2013. Sesquiterpenoids lactones: benefits to plants and people. *International Journal of Molecular Sciences* 14(6), 12780-12805.

Coskun, O., 2016. Separation techniques: chromatography. *Northern Clinics of Istanbul* 3(2), 156.

Costa, M.L., 2014. Cytoskeleton and adhesion in myogenesis. *ISRN Developmental Biology*. <http://dx.doi.org/10.1155/2014/713631>.

Da Silva Gasque, K.C., Al-Ahj, L.P., Oliveira, R.C. and Magalhães, A.C. 2014. Cell density and solvent are critical parameters affecting formazan evaluation in MTT assay. *Brazilian Archives of Biology and Technology* 57 (3), 381-385.

Dong, M.W., 2006. *Modern HPLC for practising scientists*, pp. 1-15, John Wiley & Sons, New Jersey.

Erhirhie, E.O., Ihekwereme, C.P. and Ilodigwe, E.E., 2018. Advances in acute toxicity testing: strengths, weaknesses and regulatory acceptance. *Interdisciplinary Toxicology*, 11(1), 5-12.

Fouché, G., Ackerman, L.G., Venter, E.A., Mathe, Y.Z., Liles, D.C. and Botha, C.J., 2019. Sesquiterpene lactones from *Geigeria aspera* Harv. and their cytotoxicity. *Natural Product Research*, <https://doi.org/10.1080/14786419.2019.1675068>.

Gaspar, A.R.M.D., Potgieter, D.J.J. and Vermeulen, N.M.J., 1986. The effect of the sesquiterpene lactones from *Geigeria* on glycolytic enzymes. *Biochemical Pharmacology* 35(3), 493-497.

Green, P.S. and Leeuwenburgh, C., 2002. Mitochondrial dysfunction is an early indicator of doxorubicin-induced apoptosis. *Biochimica et Biophysica Acta (BBA)- Molecular Basis of Disease*, 1588(1), 94-101.

Gonzalez, F.J. and Tukey, R.H., 2006. Drug metabolism. Goodman & Gilman's. *The Pharmacological Basis of Therapeutics*, 11th edn, pp. 71-91, McGraw-Hill, New York.

Gowrisankar, D., Abbulu, K., Bala Souri, O. and Sujana, K., 2010. Validation and calibration of analytical instruments. *Journal of Biomedical Science and Research* 2(2), 89-99.

Grosskopf, J.F.W., 1964, 'Our present knowledge of "vermeersiekte" (Geigeria poisoning)', Technical Communication 21. Department of Agricultural Technical Services. Government Printer, Pretoria, South Africa.

Gu, X., Albrecht, W., Edlund, K., Kappenberg, F., Rahnenführer, J., Leist, M., Moritz, W., Godoy, P., Cadenas, C., Marchan, R., Brecklinghaus, T., Pardom L.T., Castell, J.V., Gardner, I., Han, B., Hengstler, J.G. and Stoeber, R., 2018. Relevance of the incubation period in cytotoxicity testing with primary human hepatocytes. *Archives of Toxicology* 92 (12), 3505-3515. <https://dx.doi.org/10.1007/s00204-018-2302-0>.

Hansen, K.M.U.S.W., Bernstein, J.S.A.A.P. and McNally, M.E.P., 2015. Precision of internal standard and external standard methods in high performance liquid chromatography. <http://www.chromatographyonline.com/precision-internal-standard-and-external-standard-methods-high-performance-liquid-chromatography>.

Hostanska, K., Melzer, J., Rostock M., Suter, A. and Saller, R., 2014. Alteration of anti-inflammatory activity of *Harpagophytum procumbens* (devil's claw) extract after external metabolic activation with S9 mix. *Journal of Pharmacy and Pharmacology* 66(11), 1606-1614.

Hussien, T., El-Toumy, S., Hassan, H. and Hetta, M., 2016. Cytotoxic and antioxidant activities of secondary metabolites from *Pulicaria undulata*. *International Journal of Pharmacy and Pharmaceutical Sciences* 8(9), 150-155.

Ivanescu, B., Miron, A. and Corciova, A., 2015. Sesquiterpene lactones from *Artemisia* genus: biological activities and methods of analysis. *Journal of Analytical Methods in Chemistry*. <https://doi.org/10.1155/2015/247685>

Jia, L. and Liu, X., 2007. The conduct of drug metabolism studies considered good practice (II): *in vitro* experiments. *Current Drug Metabolism* 8(8), 822-829.

Joubert, J.P.J., 1983. Attempted prevention and treatment of *Geigeria filifolia* mattj. poisoning (vermeersiekte) in sheep. *Journal of the South African Veterinary Association* 54(4), 255-258.

Kellerman, T.S., Coetzer, J.A.W., Naudé, T.W. and Botha, C.J., 2005. *Plant poisonings and mycotoxicoses of livestock in Southern Africa*, 2nd edn, pp. 184-191, Oxford University Press, South Africa.

Kellerman, T.S., Naudé, T.W. and Fourie, N., 1996. The distribution, diagnoses and estimated economic impact of plant poisonings and mycotoxicoses in South Africa. *Onderstepoort Journal of Veterinary Research* 63, 65-90.

Litchfield, J.T. and Wilcoxon, F., 1949. A simplified method of evaluating dose–effect experiments. *Journal of Pharmacology and Experimental Therapeutics* 96(2), 99-113.

Knight, A., 2007. *A guide to poisonous house and garden plants*, 1st edn, Teton NewMedia, Jackson, Wyoming.

Kok-Yong, S. and Lawrence, L., 2015. Drug Distribution and Drug Elimination. *Basic pharmacokinetic concepts and some clinical applications*, pp. 99-116, InTech, Rijeka, Croatia.

Kuete, V., Karaosmanoglu, O. and Sivas, H., 2017. Anticancer Activities of African Medicinal Spices and Vegetables. *In Medicinal Spices and Vegetables from Africa*, pp. 271-297, Academic press, Dschang, Cameroon.

Kupchan, S.M., Eakin, M.A. and Thomas, A.M., 1971. Tumor inhibitors. 69. Structure-cytotoxicity relations among the sesquiterpene lactones. *Journal of Medicinal Chemistry* 14(12), 1147-1152.

Kuznetsova, A.V., Javadov, S., Sickinger, S., Frotschnig, S. and Grimm, M., 2015. H9c2 and HL-1 cells demonstrate distinct features of energy metabolism, mitochondrial function and sensitivity to hypoxia-reoxygenation. *Biochimica Biophysica Acta - Molecular Cell Research* 1853(2), 276–284. DO:[10.1016/j.bbamcr.2014.11.015](https://doi.org/10.1016/j.bbamcr.2014.11.015).

Lim, C.K. and Lord, G., 2002. Current developments in LC-MS for pharmaceutical analysis. *Biological and Pharmaceutical Bulletin* 25(5), 547-557.

Méry, B., Guy, J.B., Vallard, A., Espenel, S., Ardail, D., Rodriguez-Lafrasse, C., Rancoule, C. and Magné, N., 2017. *In vitro* cell death determination for drug discovery: A landscape review of real issues. *Journal of Cell Death*, <https://doi.org/10.1177%2F1179670717691251>.

Meyer, H.J. and Van Staden, J., 1986. *In vitro* culture of *Geigeria aspera* Harv. *Plant Cell, Tissue and Organ Culture* 5(3), 205-211.

Meyer, H.J. and Van Staden, J., 1989. *Geigeria aspera* Harv.: *in vitro* culture and medicinal value of sesquiterpene lactones. In *Medicinal and Aromatic Plants II*, pp. 227-245, Springer, Berlin, Heidelberg.

Moldoveanu, S.C. and David, V., 2013. *Essentials in modern HPLC separations*, pp. 1-69, Elsevier publications, United States of America.

Moosavi, S.M. and Ghassabian, S., 2018. Linearity of Calibration Curves for Analytical Methods: A Review of Criteria for Assessment of Method Reliability. *Calibration and Validation of Analytical Methods: A Sampling of Current Approaches*, pp.109-127, IntechOpen Limited, London, United Kingdom.

Mossman, T., 1983. Rapid colorimetric assay for cellular growth and survival: application to proliferation and cytotoxicity assays. *Journal of Immunological Methods* 65(1-2), 55-63.

Motulsky, H. and Christopoulos, A., 2004. *Fitting models to biological data using linear and nonlinear regression: a practical guide to curve fitting*, 1st edn, Oxford University Press, New York, United States of America.

Nagy, G., Peng, T. and Pohl, N.L., 2017. Recent liquid chromatographic approaches and developments for the separation and purification of carbohydrates. *Analytical Methods* 9(24), 3579-3593.

Narasimhan, T. R., Kim, H.L. and Safe, S.H., 1989. Effects of sesquiterpene lactones on mitochondrial oxidative phosphorylation. *General Pharmacology* 20(5), 681-687.

Nickien, M., Heuwerkerk, A., Ito, K. and van Donkelaar, C. C., 2018. Comparison between *in vitro* and *in vivo* cartilage overloading studies based on a systematic literature review. *Journal of Orthopaedic Research* 36(8), 2076-2086.

Ogu, C.C. and Maxa, J.L., 2000, October. Drug interactions due to cytochrome P450. In *Baylor University Medical Center Proceedings* 13 (4), 421-423.

Padilla-Gonzalez, G.F., dos Santos, F.A. and Da Costa, F.B., 2016. Sesquiterpene lactones: more than protective plant compounds with high toxicity. *Critical Reviews in Plant Sciences* 35(1), 18-37.

Papadimitriou, D., Xanthos, T., Dontas, I., Lelovas, P. and Perrea, D. 2008. The use of mice and rats as animal models for cardiopulmonary resuscitation research. *Laboratory Animals* 42, 265–276. DOI: [10.1258/la.2007.006035](https://doi.org/10.1258/la.2007.006035).

Park, S-Y., Gifford, J. R., Andtbacka, R.H.I., Trinity, J. D., Hynstrom, J.R., Garten, R.S., Diakos, N.A., Ives, S.J., Dela, F., Larsen, S., Drakos, S. and Richardson, R.S., 2014. Cardiac, skeletal, and smooth muscle mitochondrial respiration: are all mitochondria created equal? *American Journal of Physiology: Heart and Circulatory Physiology* 307(3), 346–352. DOI: [10.1152/ajpheart.00227.2014](https://doi.org/10.1152/ajpheart.00227.2014).

Patnaik, P., 2007. *A comprehensive guide to the hazardous properties of chemical substances*, 3rd edn, pp. 17-25, John Wiley & Sons, Canada.

Payne, R. A., 2017. *Guide to regression, nonlinear and generalized linear models*, 19th edn, VSN International, Hemel Hempstead, United Kingdom. Web page: GenStat.co.uk.

Penrith, M.L., Botha, C.J. and Tustin, R.C., 2015. Plant poisonings in livestock in Brazil and South Africa. *Journal of the South African Veterinary Association* 86(1), 01-03.

Petrova, O.E. and Sauer, K., 2017. High-performance liquid chromatography (HPLC)-based detection and quantitation of cellular c-di-GMP. In *c-di-GMP Signalling*, pp. 33-43, Humana Press, New York.

Picman, A.K., 1986. Biological activities of sesquiterpene lactones. *Biochemical Systematics and Ecology* 14(3), 255-281.

Pienaar, J.G., Kriek, N.P.J., Naude, T.W., Adelaar, T.F. and Ellis, S.D., 1973. 'Lesions in sheep skeletal and oesophageal muscle in vermeersiekte (*Geigeria ornativa* O. Hoffm. poisoning)', *Onderstepoort Journal of Veterinary Research* 40(3), 127-137.

Retief, E. 2003. *Geigeria*. In G. Germishuizen and N.L. Meyer (eds), *Plants of southern Africa: an annotated checklist*, pp. 229-231, National Botanical Institute, Pretoria.

Rimington, C. and Roets, G.C.S., 1936. Chemical studies upon the vermeerbos, *Geigeria aspera* Harv. I. Isolation of a bitter principle "geigerin". *Onderstepoort Journal of Veterinary Science and Animal Industry* 7, 485–506.

Rimington, C. Roets, G.C.S., Steyn, D.G. and Du Toit, P.J., 1936. Chemical studies upon the Vermeerbos, *Geigeria aspera*, Harv. II. Isolation of the active principle "vermeeric acid". *Onderstepoort Journal of Veterinary Science and Animal Industry* 7, 507-520
<http://hdl.handle.net/2263/60764>.

Roberts, S.M., James, R.C. and Williams, P.L., 2014. *Principles of toxicology: environmental and industrial applications*, pp. 34-333, John Wiley & Sons.

Rodriguez, E., Towers, G.H.N. and Mitchell, J.C., 1976. Biological activities of sesquiterpene lactones. *Phytochemistry* 15(11), 1573-1580.

Rossi, C., Ambrogi, V., Grandolini, G., Scarcia, V. and Furlani, A., 1986. Synthesis and *in vitro* cytotoxic activity of semisynthetic derivatives in the santonin series. *Journal of Pharmaceutical Sciences* 75(8), 784-786.

Seca, A.M.L., Silva, A.M.S. and Pinto, D.C.G.A., 2017. Parthenolide and parthenolide-like sesquiterpene lactones as multiple targets drugs: current knowledge and new developments. Atta-Ur-Rahman (eds), *Studies in Natural Products Chemistry (Bioactive Natural Products)*, pp. 337-372. Elsevier Science Publishers, Amsterdam, Netherlands.

Snyman, L.D., Carstens, A., Schultz, R.A., Joubert, J.P.J. and Labuschagne, L., 2008. Changes in sheep oesophageal diameter and function during *Geigeria ornativa* (vermeerbos) poisoning and subsequent recovery. *Journal of the South African Veterinary Association* 79(4), 178-184.

Snyman, L.D., Schultz, R.A., Kellerman, T.S. and Labuschagne, L., 2002. Continuous exposure to an aversive mixture as a means of maintaining aversion to vermeerbos (*Geigeria ornativa* O. Hoffm.) in the presence of non-averted sheep. *Onderstepoort Journal of Veterinary Research* 69, 321-325.

Stavropoulou, E., Pircalabioru, G.G. and Bezirtzoglou, E., 2018. The role of cytochromes P450 in infection. *Frontiers in Immunology* 9, 89-90. [https://doi: 10.3389/fimmu.2018.00089](https://doi.org/10.3389/fimmu.2018.00089).

Steyn, D.G., 1930. Vermeersiekte. *Journal of the South African Veterinary Association* 1(4), 31-36.

Steyn, D.G., 1934. The toxicology of plants in South Africa. *Onderstepoort Journal of Veterinary Science and Animal Industry* 3(2), 385.

Strober, W., 1997. Trypan blue exclusion test of cell viability. *Current Protocols in Immunology* 21(1), A-3B.

Szultka-Mlynska, M. and Buszewski, B., 2016. Study of *in vitro* metabolism of selected antibiotic drugs in human liver microsomes by liquid chromatography coupled with tandem mass spectrometry. *Analytical and Bioanalytical Chemistry* 408(29), 8273-8287.

Taxak, N. and Bharatam, P.V., 2014. Drug metabolism. *Resonance* 19(3), 259-282.

Tsai, T-Y., Chan, P., Gong, C-L., Wong, K-L., Su, T-H., Shen, P-C., Leung, Y-M. and Liu, Z-M. 2015. Parthenolide-induced cytotoxicity in H9c2 cardiomyoblasts involves oxidative stress. *Acta Cardiologica Sinica* 31, 33-41. DOI: [10.6515/ACS20140422B](https://doi.org/10.6515/ACS20140422B).

Timbrell, J.A., 2008. *Principles of biochemical toxicology*, 4th edn, pp. 35-126, CRC Press, New York, United States of America.

Vahrmeijer, J., 1981. *Poisonous plants of southern Africa that cause stock losses*. Tafelberg Publishers Limited, Cape Town, South Africa.

Van Aswegen, C.H., Vermeulen, N.M.J. and Potgieter, D.J.J., 1979. Inhibition of oxidative phosphorylation by sesquiterpene lactones from *Geigeria aspera*. *South African Journal of science* 75 (2), 84–85.

Van Aswegen, C., Vermeulen, N. and Potgieter, D., 1982. Site of respiratory inhibition by sesquiterpene lactones from *Geigeria*. In *South African Journal of Science* 78 (9), 374-374.

Vogelzang, M.E., Vermeulen, N.M.J., Potgieter D.J.J. and Strauss H.F., 1978. Ivalin in *Geigeria aspera*. *Phytochemistry* 17(11), 2030–2031.

Van der Lugt, J.J. and Van Heerden, J., 1993. Experimental vermeersiekte (*Geigeria ornativa* O. Hoffm. poisoning) in sheep. II: Histological and ultrastructural lesions. *Journal of the South African Veterinary Association* 64(2), 82.

Van Heerden, J., Van der Lugt, J.J. and Durante E., 1993. Experimental vermeersiekte (*Geigeria ornativa* O. Hoffm. poisoning) in sheep. I: An evaluation of diagnostic aids and an assessment of the preventive effect of ethoxyquin. *Journal of the South African Veterinary Association* 64(2), 76-81.

Weon, J.B., Ma, J.Y., Yang, H.J., Lee, B., Yun, B.R. and Ma, C.J., 2013. Qualitative and quantitative analysis of nine major compounds in the Bozhougyiqi-Tang using a high-performance liquid chromatography coupled with a diode array detector and electrospray ionization mass spectrometer. *Pharmacognosy Magazine* 9(35), 271.

Wu, W.N. and McKown, L.A., 2004. *In vitro* drug metabolite profiling using hepatic S9 and human liver microsomes. In *Optimization in Drug Discovery*, pp. 163-184, Humana Press, Totowa, New Jersey.